Huang et al. Nanoscale Research Letters (2016) 11:247
DOI 10.1186/s11671-016-1463-0

Nanoscale Research Letters

NANO EXPRESS Open Access

Suppression of Breast Cancer Cell Migration by Small Interfering RNA Delivered by Polyethylenimine-Functionalized Graphene Oxide

Yuan-Pin Huang[1], Chao-Ming Hung[2], Yi-Chiang Hsu[3,4], Cai-Yan Zhong[5], Wan-Rou Wang[5], Chi-Chang Chang[6] and Mon-Juan Lee[4,5*]

Abstract

The carbon-based nanomaterial graphene can be chemically modified to associate with various molecules such as chemicals and biomolecules and developed as novel carriers for drug and gene delivery. In this study, a nonviral gene transfection reagent was produced by functionalizing graphene oxide (GO) with a polycationic polymer, polyethylenimine (PEI), to increase the biocompatibility of GO and to transfect small interfering RNA (siRNA) against C-X-C chemokine receptor type 4 (CXCR4), a biomarker associated with cancer metastasis, into invasive breast cancer cells. PEI-functionalized GO (PEI-GO) was a homogeneous aqueous solution that remained in suspension during storage at 4 °C for at least 6 months. The particle size of PEI-GO was 172 ± 4.58 and 188 ± 5.00 nm at 4 and 25 °C, respectively, and increased slightly to 262 ± 17.6 nm at 37 °C, but remained unaltered with time. Binding affinity of PEI-GO toward siRNA was assessed by electrophoretic mobility shift assay (EMSA), in which PEI-GO and siRNA were completely associated at a PEI-GO:siRNA weight ratio of 2:1 and above. The invasive breast cancer cell line, MDA-MB-231, was transfected with PEI-GO in complex with siRNAs against CXCR4 (siCXCR4). Suppression of the mRNA and protein expression of CXCR4 by the PEI-GO/siCXCR4 complex was confirmed by real-time PCR and western blot analysis. In addition, the metastatic potential of MDA-MB-231 cells was attenuated by the PEI-GO/siCXCR4 complex as demonstrated in wound healing assay. Our results suggest that PEI-GO is effective in the delivery of siRNA and may contribute to targeted gene therapy to suppress cancer metastasis.

Keywords: Graphene oxide (GO), Polyethylenimine (PEI), Small interfering RNA (siRNA), C-X-C chemokine receptor type 4 (CXCR4), Cancer cell migration

Background

Graphene oxide (GO) is a carbon-based nanomaterial with a single layer of carbon molecules covalently linked to oxidized functional groups such as carboxyl (–COOH) and hydroxyl (–OH) groups, which can be chemically modified to increase its biocompatibility in order to associate with drugs and biomolecules [1]. Functionalized graphene oxide has been considered nanocarriers for drug delivery [2–4], gene delivery [5–8], combined delivery of drug and gene for cancer therapy [9–12], as well as protein transportation [13–15]. It has also been applied in biosensing [16, 17], bioimaging [18, 19], and tissue engineering [20, 21].

Polyethylenimine (PEI), a polycationic polymer that attracts nucleic acids through electrostatic interaction, is commonly used in the functionalization of nanomaterials for gene delivery. PEI-functionalized GO (PEI-GO) successfully delivered both small interfering RNA (siRNA) and anticancer drugs to enhance chemotherapeutic effect in cancer cells [9]. A noncovalent PEI-GO complex was reported to enhance GFP plasmid expression in HeLa cells [22]. By exploiting the near-infrared

* Correspondence: mjlee@mail.cjcu.edu.tw
[4]Innovative Research Center of Medicine, Chang Jung Christian University, Tainan, Taiwan
[5]Department of Bioscience Technology, Chang Jung Christian University, No. 1 Changda Rd., Gueiren District, Tainan City 71101, Taiwan
Full list of author information is available at the end of the article

(NIR) optical absorbance of GO, photothermally controlled delivery of siRNA and plasmid DNA by GO functionalized with both PEI and polyethylene glycol (PEG) was achieved [23, 24].

Chemokine (C-X-C motif) receptor 4 (CXCR4), which is a class-A G protein-coupled receptor (GPCR), has been considered a biomarker for cancer metastasis and poor prognosis [25, 26]. Suppression of CXCR4 and its signaling axis is therefore a common strategy to inhibit cancer cell migration and metastasis [27–30]. Drug and gene delivery systems based on nanomaterials are thus designed to target against CXCR4 and facilitate cancer therapy and imaging. Anti-CXCR4 monoclonal antibody conjugated to superparamagnetic nanoparticles was applied in molecular imaging of pancreatic cancer cell lines [31]. PEG-functionalized carbon nanotube and cationic dextran-based nanoparticles were reported to deliver siRNA against CXCR4 into primary cells and animal model for colorectal cancer [32, 33]. Peptide ligands and peptide dendrimers against CXCR4 were used alone or in conjugation with nanoparticles to deliver anticancer drugs, inhibit tumor metastasis, and enhance molecular imaging [34–37]. In addition, synthetic polycationic viologen dendrimers (VGD) targeting CXCR4 were also developed to facilitate targeted delivery of plasmid DNAs and cancer therapy [38].

In this study, we explored the potential of PEI-GO in the transfection of siRNAs against CXCR4 (siCXCR4) to suppress the migration of MDA-MB-231 cells, a metastatic cancer cell line overexpressing CXCR4. Transfection efficiency was evaluated by the level of suppression of CXCR4 mRNA, as well as the migration ability of MDA-MB-231, and was compared to a commercial transfection reagent, Lipofectamine 2000. Our results suggest that PEI-GO is a potentially efficient nonviral transfection reagent that may contribute to targeted cancer therapy.

Methods

PEI Functionalization of Graphene Oxide

Graphene oxide (GO, Sigma-Aldrich, St. Louis, MO, USA) was activated with (1-ethyl-3-(3-dimethyl-aminopropyl) carbodiimide (EDC) and linked to PEI (branched, average M_W~25,000 by LS, average M_n~10,000 by GPC, Sigma-Aldrich, St. Louis, MO, USA) through the formation of amide bonds (–CONH–) using methods reported in the literature [9]. To remove unbound PEI, the reaction product was washed with ddH_2O and centrifuged repeatedly at 3,000 rpm for 15–30 min in an Amicon Ultra-15 Centrifugal Filter Unit (Millipore, Billerica, MA, USA) with a molecular weight cut-off of 100 kDa. The flow-through was subjected to ninhydrin assay to determine the level of free PEI.

Ninhydrin Assay

During washing of PEI-GO, 1 ml of flow-through from the Amicon Ultra-15 Centrifugal Filter Unit was mixed with 200 μl of 2 % (*w*/*v*) ninhydrin solution, followed by reaction in a boiling water bath for 3 min. Ninhydrin reacts with the primary and secondary amines of free PEI to produce Ruhemann's purple, which was gradually decreased with successive washing. PEI-GO was considered

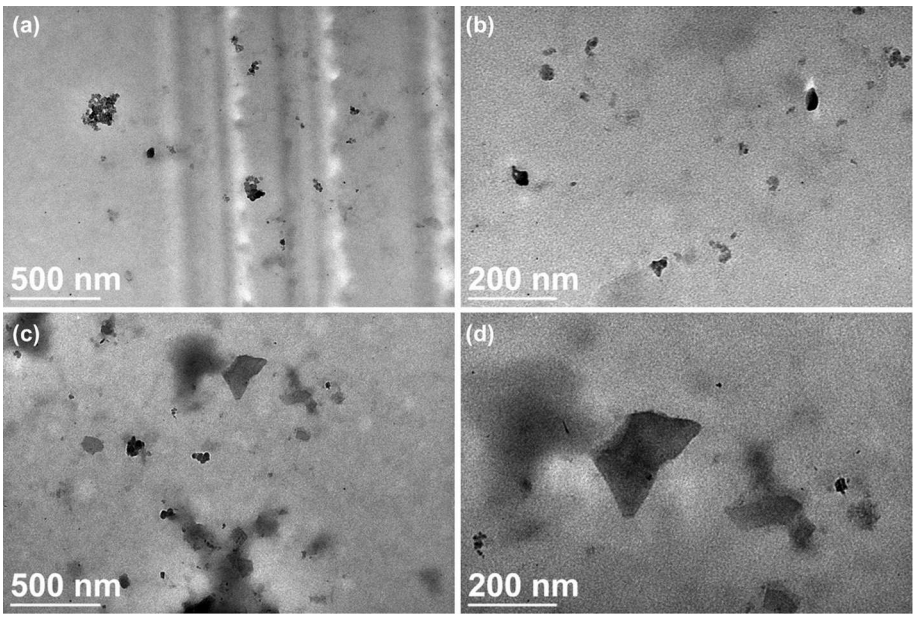

Fig. 1 Transmission electron microscopy images of pristine GO and PEI-GO. The surface morphology of pristine GO (**a**, **b**) was compared with that of PEI-GO (**c**, **d**) by a JEOL 2000FX TEM at different scales

free of unreacted PEI when the color of Ruhemann's purple was undetectable by the naked eye.

Characterization of PEI-GO

The difference in morphology between pristine GO and PEI-GO was examined by transmission electron microscopy (JEOL 2000FX TEM) and scanning electron microscopy (JSM-6500F SEM). The particle size and zeta potential of PEI-GO were determined by dynamic light scattering using Zetasizer Nano ZS system (Malvern Instruments, Worcestershire, UK).

Electrophoretic Mobility Shift Assay (EMSA)

Dharmacon siGENOME GAPD Control siRNA (Thermo Fisher Scientific, Waltham, MA, USA) was used in EMSA to analyze the binding capacity of PEI-GO. The PEI-GO:siRNA complex was formed by incubating 0–0.6 μg of PEI-GO with 0.2 μg siRNA at various mass ratios in serum-free cell culture medium for 20 min at room temperature. The complex was then mixed with SYBR Green I and resolved by 1 % agarose gel as described previously [39].

Cell Culture

Human breast carcinoma cell line MDA-MB-231 was cultured at 37 °C in the absence of CO_2 in Leibovitz's L-15 medium (Gibco, Life Technologies, Carlsbad, CA, USA) supplemented with 10 % fetal bovine serum (FBS), 50 units/ml penicillin, and 50 μg/ml streptomycin. The medium was refreshed every 3–4 days, and confluent cells were subcultured 7 days after seeding. Cells were seeded at 5000 cells/well in 96-well plates for cell viability assay, at 10^5 cells/well in 6-well plates for total RNA extraction, and at 2×10^4 cells/well in 24-well plates for wound healing assay.

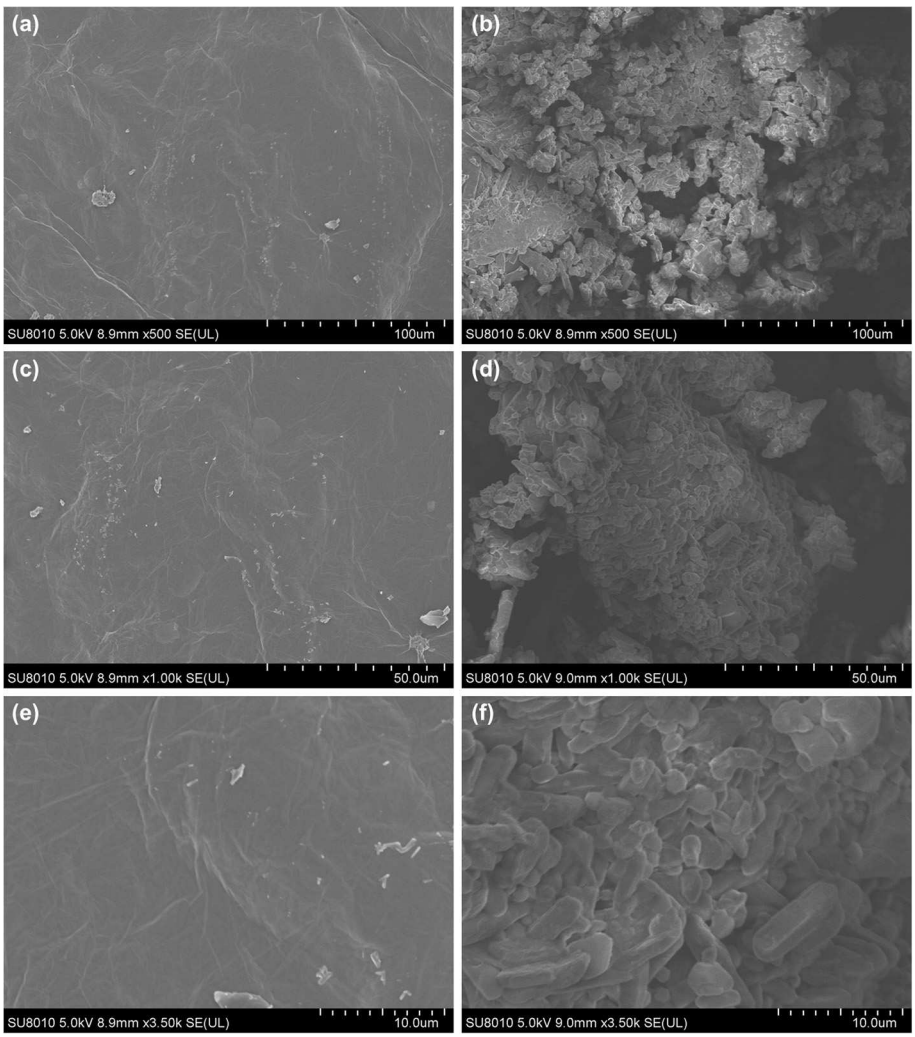

Fig. 2 Scanning electron microscopy images of pristine GO and PEI-GO. The surface morphology of pristine GO (**a**, **c**, **e**) was compared with that of PEI-GO (**b**, **d**, **f**) by a JSM-6500 F SEM at different scales

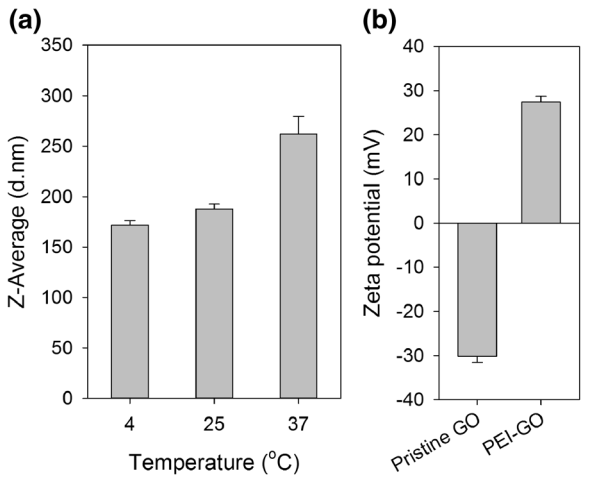

Fig. 3 Average particle size and zeta potential of PEI-GO analyzed by dynamic light scattering. **a** The average particle diameter of 1 mg/ml PEI-GO was compared at 4, 25, and 37 °C. **b** The zeta potential of 1 mg/ml PEI-GO was compared to that off pristine GO at 25 °C and neutral pH. *Error bars* represent standard deviations ($n \geq 3$)

Cell Viability Assay

MDA-MB-231 cells were treated with 0–20 μg/ml PEI-GO for 48 h, followed by WST-1 assay using Quick Cell Proliferation Colorimetric Assay Kit (BioVision, Milpitas, CA, USA). Cell viability was quantitated spectrophotometrically by measuring the optical density at 450 nm, with a reference wavelength of 650 nm.

siRNA Transfection with PEI-GO

MDA-MB-231 cells were treated with Dharmacon siGENOME siRNA specific for human CXCR4 (siCXCR4) or siGENOME GAPD Control siRNA (siMOCK). The siRNA was delivered either by Lipofectamine 2000 (Life Technologies, Carlsbad, CA, USA) according to manufacturer's instructions or by PEI-GO. PEI-GO was incubated with siCXCR4 at mass ratios of 0.3:1, 0.5:1, and 1:1 for 20 min at room temperature before cultured with MDA-MB-231 cells to achieve a final siCXCR4 concentration of 25 nM. Two days after siRNA transfection, cells were harvested for RNA extraction and real-time PCR analysis or subjected to wound healing assay.

Real-Time Polymerase Chain Reaction

Total RNA was isolated by PureLink® RNA Mini Kit (Thermo Fisher Scientific, Waltham, MA, USA), and cDNA synthesis was carried out using the SuperScript III First-Strand Synthesis SuperMix for qRT-PCR (Life Technologies, Carlsbad, CA, USA) according to the manufacturer's instructions. The cDNA was diluted to a final concentration of ~1 ng/μl and reacted with CXCR4 (NM_003467)- or GAPDH (NM_002046.4)-specific primer pairs and QuantiFast SYBR® Green PCR Kit (QIAGEN, Germantown, MD, USA). PCR was performed by Applied Biosystems 7300 Real-Time PCR System and monitored with Applied Biosystems Sequence Detection Software V1.2 (Life Technologies, Carlsbad, CA, USA) as described previously [40].

Wound Healing Assay

Wound healing assay was performed by following the protocol provided in the literature [41]. MDA-MB-231 cells were cultured in a 24-well plate and treated with siCXCR4 or siMOCK complexed with either PEI-GO or Lipofectamine 2000 for 48 h. The cell monolayer in each well was scraped with a p200 pipet tip to create a gap. After washing with culture medium to remove cell debris, the cells were allowed to migrate for 24 h, followed by observation under an Olympus CKX41 optical microscope.

Statistical Analysis

Statistical analysis was performed on data from at least three independent experiments. Significant difference relative to the control was tested using Student's t test. Levels of significance of $p < 0.05$ and 0.01 were accepted as significant and highly significant, respectively.

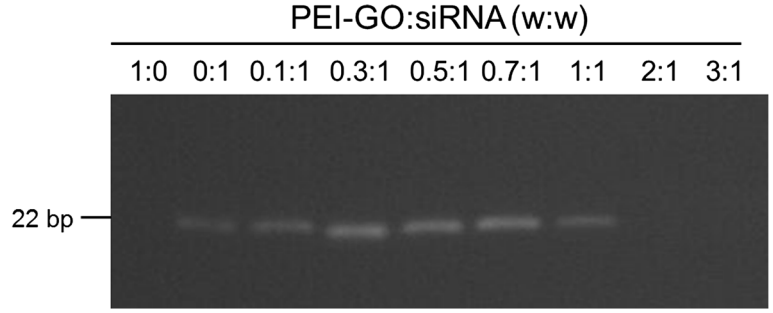

Fig. 4 Binding capacity of PEI-GO toward siRNA. PEI-GO was reacted with Dharmacon siGENOME GAPD control siRNA at various mass ratios, followed by electrophoretic mobility shift assay (EMSA)

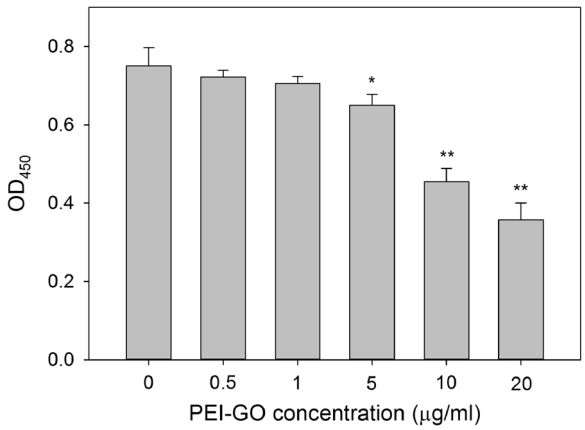

Fig. 5 Cytotoxicity of PEI-GO in MDA-MB-231 cells. Human breast carcinoma cells MDA-MB-231 were treated with 0–20 μg/ml of PEI-GO for 48 h. Cell viability was determined by WST-1 assay and quantitated spectrophotometrically by measuring the optical density at 450 nm, with a reference wavelength of 650 nm. *Error bars* represent standard deviations ($n \geq 3$). *$p < 0.05$ and **$p < 0.01$ compared to the control

Results

Characterization of PEI-GO

PEI functionalization increased the hydrophilicity and dispersibility of GO, which formed aggregates and precipitated in water prior to functionalization. The PEI-GO suspension can be maintained for at least 10 months without precipitation. As examined by transmission electron microscopy and scanning electron microscopy, pristine GO was tightly packed (Fig. 1a, b) and had a relatively smooth surface (Fig. 2a, c, e). PEI functionalization increased the surface area of PEI-GO, as well as the spacing between graphene layers, which appeared more extended (Fig. 1c, d) and was highly agglomerated, indicating that the stacking of the graphene sheets was disturbed (Fig. 2b, d, f). The particle size of PEI-GO was 172 ± 4.58 and 188 ± 5.00 nm at 4 and 25 °C, respectively, and increased slightly to 262 ± 17.6 nm at 37 °C (Fig. 3a), suggesting that that PEI-GO may be partially aggregated in cell culture. However, when the particle size immediately after synthesis was compared to that after stored at 4 °C for over 10 months, no significant change was observed (data not shown). As shown in Fig. 3b, the zeta potential of pristine GO was negative (−30.2 ± 1.34 mV), while that of PEI-GO was positive (27.4 ± 1.25 mV), indicating that PEI functionalization increased the positive charge on the surface of GO and contributed to the electrostatic repulsion that stabilized the PEI-GO suspension.

Binding Capacity of PEI-GO to siRNA

Binding capacity of PEI-GO toward siRNA was assessed by electrophoretic mobility shift assay (EMSA). PEI-GO was complexed with siRNA at various mass ratios and resolved with agarose gel electrophoresis (Fig. 4). Binding of siRNA to PEI-GO resulted in reduced mobility of free siRNAs and their availability for SYBR Green I intercalation. As the amount of PEI-GO increased, more siRNAs were adsorbed, resulting in decreased fluorescence signal of free siRNAs. The migration of siRNA was completely inhibited when the mass ratio of PEI-GO:siRNA was 2:1 and above.

Cytotoxicity of PEI-GO

The cytotoxicity of PEI-GO in MDA-MB-231 cells, a invasive breast cancer cell line, was analyzed by WST-1 assay. After incubated with PEI-GO for 48 h, we observed that the viability of MDA-MB-231 cells decreased with increasing concentrations of PEI-GO (Fig. 5). In the presence of 20 μg/ml PEI-GO, the number of viable cells reduced to 47.6 % of that of the control. The final concentration of PEI-GO in siRNA transfection was therefore limited within the range which had no significant effect on cell viability.

Suppression of CXCR4 by siCXCR4 Transfected with PEI-GO

The transfection efficiency of PEI-GO compared to Lipofectamine 2000 was demonstrated by delivering siCXCR4 into MDA-MB-231 cells. After siCXCR4 treatment for

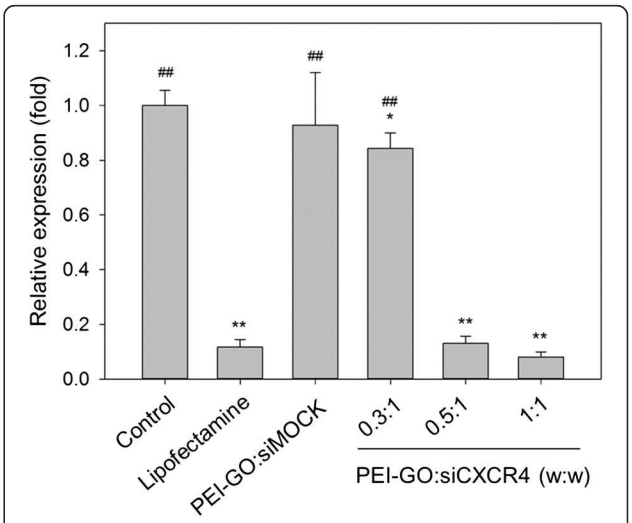

Fig. 6 Relative CXCR4 mRNA expression of MDA-MB-231 cells transfected with PEI-GO:siCXCR4 complexes. PEI-GO was incubated with siCXCR4 at mass ratios of 0.3:1, 0.5:1, and 1:1 for 20 min at room temperature before cultured with MDA-MB-231 cells to achieve a final siCXCR4 concentration of 25 nM. Two days after siRNA transfection, cells were harvested for RNA extraction and real-time PCR analysis. Control, MDA-MB-231 cells cultured in growth medium for 48 h; Lipofectamine, MDA-MB-231 cells transfected with siCXCR4 using Lipofectamine 2000 as transfection reagent; PEI-GO:siMOCK, MDA-MB-231 cells transfected with PEI-GO:siMOCK at a mass ratio of 1:1. *Error bars* represent standard deviations ($n \geq 3$). *$p < 0.05$ and **$p < 0.01$ compared to the control; $^{\#\#}p < 0.01$ compared to Lipofectamine

48 h, CXCR4 mRNA expression reduced significantly to 13 and 8 % of untreated control at PEI-GO:siCXCR4 mass ratios of 0.5:1 and 1:1, respectively, but was nearly unaffected at a PEI-GO:siCXCR4 ratio of 0.3:1, and in the presence of siMOCK, a nonspecific siRNA control (Fig. 6). Transfection efficiency of PEI-GO was comparable to that of the Lipofectamine:siCXCR4 complex, which reduced CXCR4 expression to 12 % of control. These results suggest that at appropriate mass ratios, target-specific and efficient transfection can be achieved by PEI-GO.

Effect of siCXCR4 Transfected by PEI-GO on Cell Migration

The effect of CXCR4 suppression on cell migration was examined by wound healing assay. MDA-MB-231 cells transfected with siCXCR4 were allowed to migrate in a cell-free gap created in the culture plate. For untreated cells or those treated with siMOCK, the gap was filled with migrated cells after 24 h (Fig. 7a, c). When the mRNA expression of CXCR4 was suppressed by siCXCR4, fewer cells were present in the gap, indicating that cell migration was retarded. As shown in Fig. 7d–f, siCXCR4 delivered by PEI-GO suppressed the migration of MDA-MB-231 cells at PEI-GO:siCXCR4 ratios of 0.5:1 and 1:1, but the effect was insignificant when the PEI-GO:siCXCR4 ratio was 0.3:1, consistent with the results of CXCR4 gene expression (Fig. 6). In addition, the extent of migrational suppression resulted from PEI-GO:siCXCR4 was comparable to that of the Lipofectamine:siCXCR4 complexes (Fig. 7g).

Discussion

With improved vector designs, recent clinical trials have eliminated the safety concerns of gene therapy and demonstrated remarkable therapeutic benefits in inherited diseases of the blood and immune and nervous systems [42]. Gene therapy is expected to become a new approach to the development of novel therapeutic strategies beyond conventional methods. Although current strategies on clinical gene therapy are based predominantly on viral vectors, nonviral transfection reagents provide safer alternatives without potential side effects such as immunogenicity and carcinogenesis that are associated with viral transfection [43].

In this study, we demonstrated that PEI-GO is an effective nonviral carrier for siRNA delivery and may potentially be applied in targeted gene therapy to suppress cancer metastasis. Interestingly, studies have shown that pristine graphene or GO, as well as polyethylene glycol (PEG)-modified GO (PEG-GO) inhibit breast cancer cell migration through impairment of oxidative phosphorylation and mitochondrial respiration [44, 45]. In addition, GO selectively targets and retards the clonal expansion of multiple cancer stem cells [46]. These results indicate that GO alone is capable of suppressing cancer metastasis and tumor development. However, because a relatively lower concentration of PEI-GO was used in this study (0.3 μg/ml PEI-GO compared to 40 or 80 μg/ml PEG-GO in the literature), inhibition of cell migration was not observed when MDA-MB-231 cells were treated with PEI-GO alone.

Conclusions

Our results indicate that PEI-GO is capable of delivering siCXCR4 to suppress gene expression and metastatic potential of MDA-MB-231 cells. PEI-GO may be developed as a novel nonviral transfection reagent that contributes to targeted gene therapy to suppress cancer metastasis.

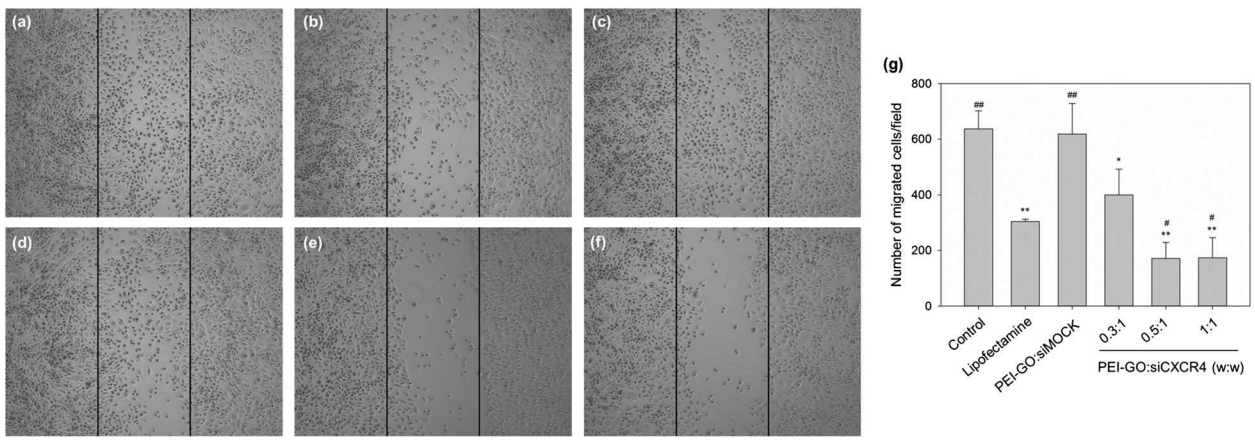

Fig. 7 Wound healing assay of MDA-MB-231 cells transfected with PEI-GO:siCXCR4 complexes. MDA-MB-231 cells were allowed to migrate over a cell-free gap (bordered by the pair of black lines) after treated with PEI-GO:siCXCR4 complexes of mass ratios 0.3:1 (**d**), 0.5:1 (**e**), and 1:1 (**f**) for 48 h. The results were compared with untreated cells (**a**) and those treated with Lipofectamine 2000:siCXCR4 (**b**) or PEI-GO:siMOCK (**c**). Migrated cells per field from three independent experiments were quantitated as shown in the bar graph (**g**)

Competing Interests
The authors declare that they have no competing interests.

Authors' Contributions
YPH was responsible for the study design and characterization of PEI-GO. CYZ and WRW synthesized PEI-GO and performed the bioassays. CMH, YCH, and CCC participated in data analysis and interpretation. MJL conceived of the study, participated in its design and coordination, and drafted and finalized the manuscript. All authors read and approved the final manuscript.

Acknowledgements
This research is supported by the Ministry of Science and Technology, Taiwan (MOST 101-2314-B-309-001-MY3 and MOST 103-2633-B-309-001), and E-Da Hospital, Kaohsiung, Taiwan (EDAHP103003 and EDAHP 104002). The authors thank Dr. Chih-Hsiang Lin and Dr. Yun-Ming Chang for their assistance in SEM and TEM imaging.

Author details
[1]Department of Cosmetics and Fashion Styling, Cheng Shiu University, Kaohsiung, Taiwan. [2]Department of General Surgery, E-Da Hospital, Kaohsiung, Taiwan. [3]Graduate Institute of Medical Sciences, Chang Jung Christian University, Tainan, Taiwan. [4]Innovative Research Center of Medicine, Chang Jung Christian University, Tainan, Taiwan. [5]Department of Bioscience Technology, Chang Jung Christian University, No. 1 Changda Rd., Gueiren District, Tainan City 71101, Taiwan. [6]Department of Obstetrics and Gynecology, E-Da Hospital, Kaohsiung, Taiwan.

Received: 3 March 2016 Accepted: 3 May 2016
Published online: 12 May 2016

References

1. Zhou X, Liang F (2014) Application of graphene/graphene oxide in biomedicine and biotechnology. Curr Med Chem 21:855–69
2. Liu J, Cui L, Losic D (2013) Graphene and graphene oxide as new nanocarriers for drug delivery applications. Acta Biomater 9:9243–57
3. Zhang L, Xia J, Zhao Q, Liu L, Zhang Z (2010) Functional graphene oxide as a nanocarrier for controlled loading and targeted delivery of mixed anticancer drugs. Small 6:537–44
4. Liu Z, Robinson JT, Sun X, Dai H (2008) PEGylated nanographene oxide for delivery of water-insoluble cancer drugs. J Am Chem Soc 130:10876–7
5. Yin D, Li Y, Lin H, Guo B, Du Y, Li X et al (2013) Functional graphene oxide as a plasmid-based Stat3 siRNA carrier inhibits mouse malignant melanoma growth in vivo. Nanotechnology 24:105102
6. Imani R, Emami SH, Faghihi S (2015) Synthesis and characterization of an octaarginine functionalized graphene oxide nano-carrier for gene delivery applications. Phys Chem Chem Phys 17:6328–39
7. Paul A, Hasan A, Kindi HA, Gaharwar AK, Rao VT, Nikkhah M et al (2014) Injectable graphene oxide/hydrogel-based angiogenic gene delivery system for vasculogenesis and cardiac repair. ACS Nano 8:8050–62
8. Yang X, Niu G, Cao X, Wen Y, Xiang R, Duana H et al (2012) The preparation of functionalized graphene oxide for targeted intracellular delivery of siRNA. J Mater Chem 22:6649–54
9. Zhang L, Lu Z, Zhao Q, Huang J, Shen H, Zhang Z (2011) Enhanced chemotherapy efficacy by sequential delivery of siRNA and anticancer drugs using PEI-grafted graphene oxide. Small 7:460–4
10. Bao H, Pan Y, Ping Y, Sahoo NG, Wu T, Li L et al (2011) Chitosan-functionalized graphene oxide as a nanocarrier for drug and gene delivery. Small 7:1569–78
11. Zhi F, Dong H, Jia X, Guo W, Lu H, Yang Y et al (2013) Functionalized graphene oxide mediated adriamycin delivery and miR-21 gene silencing to overcome tumor multidrug resistance in vitro. PLoS One 8:e60034
12. Cao X, Zheng S, Zhang S, Wang Y, Yang X, Duan H et al (2015) Functionalized Graphene Oxide with Hepatocyte Targeting as Anti-Tumor Drug and Gene Intracellular Transporters. J Nanosci Nanotechnol 15:2052–9
13. Kim S, Ryoo SR, Na HK, Kim YK, Choi BS, Lee Y et al (2013) Deoxyribozyme-loaded nano-graphene oxide for simultaneous sensing and silencing of the hepatitis C virus gene in liver cells. Chem Commun (Camb) 49:8241–3
14. Jana B, Mondal G, Biswas A, Chakraborty I, Saha A, Kurkute P et al (2013) Dual functionalized graphene oxide serves as a carrier for delivering oligohistidine- and biotin-tagged biomolecules into cells. Macromol Biosci 13:1478–84
15. Shen H, Liu M, He H, Zhang L, Huang J, Chong Y et al (2012) PEGylated graphene oxide-mediated protein delivery for cell function regulation. ACS Appl Mater Interfaces 4:6317–23
16. Wang Y, Li Z, Hu D, Lin CT, Li J, Lin Y (2010) Aptamer/graphene oxide nanocomplex for in situ molecular probing in living cells. J Am Chem Soc 132:9274–6
17. Zhang J, Sun Y, Xu B, Zhang H, Gao Y, Zhang H et al (2013) A novel surface plasmon resonance biosensor based on graphene oxide decorated with gold nanorod-antibody conjugates for determination of transferrin. Biosens Bioelectron 45:230–6
18. Kim H, Namgung R, Singha K, Oh IK, Kim WJ (2011) Graphene oxide-polyethylenimine nanoconstruct as a gene delivery vector and bioimaging tool. Bioconjug Chem 22:2558–67
19. Sun X, Liu Z, Welsher K, Robinson JT, Goodwin A, Zaric S et al (2008) Nano-Graphene Oxide for Cellular Imaging and Drug Delivery. Nano Res 1:203–12
20. Ku SH, Park CB (2013) Myoblast differentiation on graphene oxide. Biomaterials 34:2017–23
21. Lee WC, Lim CH, Shi H, Tang LA, Wang Y, Lim CT et al (2011) Origin of enhanced stem cell growth and differentiation on graphene and graphene oxide. ACS Nano 5:7334–41
22. Feng L, Zhang S, Liu Z (2011) Graphene based gene transfection. Nanoscale 3:1252–7
23. Kim H, Kim WJ (2014) Photothermally controlled gene delivery by reduced graphene oxide-polyethylenimine nanocomposite. Small 10:117–26
24. Feng L, Yang X, Shi X, Tan X, Peng R, Wang J et al (2013) Polyethylene glycol and polyethylenimine dual-functionalized nano-graphene oxide for photothermally enhanced gene delivery. Small 9:1989–97
25. Mukherjee D, Zhao J (2013) The Role of chemokine receptor CXCR4 in breast cancer metastasis. Am J Cancer Res 3:46–57
26. Yang P, Liang SX, Huang WH, Zhang HW, Li XL, Xie LH et al (2014) Aberrant expression of CXCR4 significantly contributes to metastasis and predicts poor clinical outcome in breast cancer. Curr Mol Med 14:174–84
27. Yu ZH, Liu T, Zhao YH, Huang YY, Gao YT (2014) Cisplatin targets the stromal cell-derived factor-1-CXC chemokine receptor type 4 axis to suppress metastasis and invasion of ovarian cancer-initiating cells. Tumour Biol 35:4637–44
28. Han AR, Lee JY, Kim HJ, Min WS, Park G, Kim SH (2015) A CXCR4 antagonist leads to tumor suppression by activation of immune cells in a leukemia-induced microenvironment. Oncol Rep 34(6):2880–8
29. Zhan Y, Zhang H, Li J, Zhang Y, Zhang J, He L (2015) A novel biphenyl urea derivate inhibits the invasion of breast cancer through the modulation of CXCR4. J Cell Mol Med 19:1614–23
30. Niu J, Huang Y, Zhang L (2015) CXCR4 silencing inhibits invasion and migration of human laryngeal cancer Hep-2 cells. Int J Clin Exp Pathol 8: 6255–61
31. He Y, Song W, Lei J, Li Z, Cao J, Huang S et al (2012) Anti-CXCR4 monoclonal antibody conjugated to ultrasmall superparamagnetic iron oxide nanoparticles in an application of MR molecular imaging of pancreatic cancer cell lines. Acta Radiol 53:1049–58
32. Abedini F, Hosseinkhani H, Ismail M, Domb AJ, Omar AR, Chong PP et al (2012) Cationized dextran nanoparticle-encapsulated CXCR4-siRNA enhanced correlation between CXCR4 expression and serum alkaline phosphatase in a mouse model of colorectal cancer. Int J Nanomedicine 7:4159–68
33. Liu Z, Winters M, Holodniy M, Dai H (2007) siRNA delivery into human T cells and primary cells with carbon-nanotube transporters. Angew Chem Int Ed Engl 46:2023–7
34. Chittasupho C, Lirdprapamongkol K, Kewsuwan P, Sarisuta N (2014) Targeted delivery of doxorubicin to A549 lung cancer cells by CXCR4 antagonist conjugated PLGA nanoparticles. Eur J Pharm Biopharm 88:529–38
35. Tarasov SG, Gaponenko V, Howard OM, Chen Y, Oppenheim JJ, Dyba MA et al (2011) Structural plasticity of a transmembrane peptide allows self-assembly into biologically active nanoparticles. Proc Natl Acad Sci U S A 108:9798–803
36. Kuil J, Buckle T, Oldenburg J, Yuan H, Borowsky AD, Josephson L et al (2011) Hybrid peptide dendrimers for imaging of chemokine receptor 4 (CXCR4) expression. Mol Pharm 8:2444–53
37. Gallo J, Kamaly N, Lavdas I, Stevens E, Nguyen QD, Wylezinska-Arridge M et al (2014) CXCR4-targeted and MMP-responsive iron oxide nanoparticles for enhanced magnetic resonance imaging. Angew Chem Int Ed Engl 53:9550–4
38. Li J, Lepadatu AM, Zhu Y, Ciobanu M, Wang Y, Asaftei SC et al (2014) Examination of structure-activity relationship of viologen-based dendrimers as CXCR4 antagonists and gene carriers. Bioconjug Chem 25:907–17

39. Huang YP, Lin IJ, Chen CC, Hsu YC, Chang CC, Lee MJ (2013) Delivery of small interfering RNAs in human cervical cancer cells by polyethylenimine-functionalized carbon nanotubes. Nanoscale Res Lett 8:267
40. Tsai YH, Lin KL, Huang YP, Hsu YC, Chen CH, Chen Y et al (2015) Suppression of ornithine decarboxylase promotes osteogenic differentiation of human bone marrow-derived mesenchymal stem cells. FEBS Lett 589:2058–65
41. Liang CC, Park AY, Guan JL (2007) In vitro scratch assay: a convenient and inexpensive method for analysis of cell migration in vitro. Nat Protoc 2:329–33
42. Naldini L (2015) Gene therapy returns to centre stage. Nature 526:351–60
43. Yin H, Kanasty RL, Eltoukhy AA, Vegas AJ, Dorkin JR, Anderson DG (2014) Non-viral vectors for gene-based therapy. Nat Rev Genet 15:541–55
44. Zhou T, Zhang B, Wei P, Du Y, Zhou H, Yu M et al (2014) Energy metabolism analysis reveals the mechanism of inhibition of breast cancer cell metastasis by PEG-modified graphene oxide nanosheets. Biomaterials 35:9833–43
45. Zhou H, Zhang B, Zheng J, Yu M, Zhou T, Zhao K et al (2014) The inhibition of migration and invasion of cancer cells by graphene via the impairment of mitochondrial respiration. Biomaterials 35:1597–607
46. Fiorillo M, Verre AF, Iliut M, Peiris-Pages M, Ozsvari B, Gandara R et al (2015) Graphene oxide selectively targets cancer stem cells, across multiple tumor types: implications for non-toxic cancer treatment, via "differentiation-based nano-therapy". Oncotarget 6:3553–62

CARBON 51 (2013) 224–235

Available at www.sciencedirect.com

SciVerse ScienceDirect

journal homepage: www.elsevier.com/locate/carbon

Functionalized graphene oxide mediated nucleic acid delivery

Sushil Kumar Tripathi [a], *Ritu Goyal* [a], *Kailash Chand Gupta* [a,b], *Pradeep Kumar* [a,*]

[a] *CSIR – Institute of Genomics and Integrative Biology, Delhi University Campus, Mall Road, Delhi 110007, India*
[b] *CSIR – Indian Institute of Toxicology Research, M.G. Marg, Lucknow 226001, UP, India*

ARTICLE INFO

Article history:
Received 18 February 2012
Accepted 18 August 2012
Available online 26 August 2012

ABSTRACT

We report a simple preparation of linear polyethylenimine-grafted graphene oxide (LP-GO) conjugates and their efficacy to transfer nucleic acids into the mammalian cells. Graphene oxide (GO), with epoxy functions on its surface, was reacted with different amounts of linear polyethylenimine (lPEI), a non-toxic polymer, to obtain three different positively charged LP-GO conjugates (LP-GO-1 to LP-GO-3), capable of interacting with negatively charged nucleic acids (gel retardation assay) and transporting them efficiently into the cells. The results show that these conjugates not only exhibited considerably higher transfection efficiency but also possessed even better cell viability than lPEI. LP-GO-2, the best system in terms of transfection efficiency, showed improved buffering capacity compared to lPEI and provided sufficient stability to bound DNA against DNase I. Further, LP-GO-2 was used for the sequential delivery of GFP specific siRNA, which resulted in ~70% suppression of the target gene expression. Intracellular trafficking using fluorescence microscopy revealed that LP-GO-2 conjugate delivered pDNA in the nucleus within 1 h of exposure. The results indicate the prospect of using these conjugates as efficient carriers of nucleic acids for future gene therapy applications.

1. Introduction

The clinical success of gene therapy critically depends on the use of efficient and safe delivery systems. This issue has been well recognized, however, it still remains a challenge even after 25 years. Although viral vectors are much more efficient than their non-viral counterparts, the former have risks of safety and immunogenicity [1]. Therefore, much attention has been directed to the design of non-viral carriers for gene delivery [2–9]. Among the cationic polymers, branched polyethylenimine (bPEI, 25 kDa) has been one of the most extensively studied cationic polymers for gene transfection due to its intrinsic proton sponge property, which helps in the efficient release of pDNA complex in the cytoplasm for nuclear translocation [10–12]. Therefore, it has been reported as gold standard in gene delivery, however, charge-associated toxicity and its ability to interact non-specifically with blood components have hampered its *in vivo* applications [13,14]. lPEI, on the other hand, is almost non-toxic to cells but due to its poor solubility in water, it displays low transfection efficiency [15,16]. In order to improve its efficacy, various modifications have been suggested [17–19]. With the advent of nanotechnology, the development of non-viral vectors in conjugation with different nanomaterials [gold nanoparticles, carbon nanotubes (CNT) and magnetic nanoparticles] has bolstered the field within the last 10 years.

In the last few years, GO has been explored for various biomedical applications, such as synthesis of polymer composites, energy-related materials, sensors, field-effect transistors, etc., due to its excellent electrical, mechanical, optical and thermal properties [20,21]. In addition, GO possesses a good biocompatibility, water dispersibility, colloidal stability and functional groups on the surface amenable to conjugation [22]. Applications of GO in drug delivery have been reported [23,24] but, a few, very recently, have documented its use in gene delivery [25–27]. It has been shown that GO does not

* *Corresponding author:* Fax: +91 11 27667471.
E-mail address: pkumar@igib.res.in (P. Kumar).
0008-6223/$ - see front matter
http://dx.doi.org/10.1016/j.carbon.2012.08.047

interact with double-stranded DNA [25]. Therefore, modifications, on its surface, are warranted to make it an efficient carrier, which can subsequently bind pDNA and deliver it to the insides of the cell for efficient gene transfection. GO possesses a variety of reactive functional groups (epoxide, –COOH and –OH), which allow its surface modification through chemical functionalization and its subsequent use in various biomedical applications [22]. Feng et al. [25] electrostatically conjugated GO with two different bPEIs (1.2 kDa and 10 kDa) and the resulting conjugates were found to possess improved cell viability and gene expression in HeLa cells in comparison to their respective native bPEIs. In another study, Chen et al. [26] have conjugated branched polyethylenimine (25 kDa) with GO through its carboxyl functions using 1-ethyl-3-[3-(dimethylaminopropyl)] carbodiimide hydrochloride (EDAC) as a condensing reagent. The conjugate could exhibit improved cell viability (~90%), however, transfection efficiency was found to be comparable to native bPEI (25 kDa). In order to further improve this strategy, Kim et al. [27], in a similar fashion, modified GO with a low molecular weight bPEI (1.8 kDa) and investigated the toxicity, transfection efficiency as well as imaging properties of the conjugates, which displayed transfection efficiency higher than that of PEI (1.8 kDa), but comparable to bPEI (25 kDa) with cell viability ~90%. All these modifications resulted in the blockage of amines on bPEI, which, in turn, reduced the toxicity of the conjugates but compromised on the transfection efficiency. Taking a cue from these studies, we attempted to improve the gene carrying capability of GO by conjugating it with a non-toxic lPEI (25 kDa) in such a manner that total number of amines remained intact for interaction with pDNA.

Here, in this study, we have demonstrated the capability of LP-GO conjugates to condense pDNA and deliver it to HEK293 and HeLa cells efficiently. We have modified the GO surface with lPEI by harnessing mainly the epoxy functionalities present on its surface. The methodology involves the reaction of secondary amines of lPEI with epoxide-functions on the surface of GO. A small series of LP-GO conjugates was prepared by varying the weight ratio of lPEI:GO [i.e., 1.5:1 (LP-GO-1), 2.5:1 (LP-GO-2) and 5:1 (LP-GO-3)]. Subsequently, these conjugates were allowed to interact with pDNA and the resulting LP-GO/pDNA complexes subjected to characterization for their size and zeta potential. The positively charged complexes were then explored for their ability to deliver genes in HEK293 and HeLa cells. Of the three formulations, LP-GO-2/DNA complex exhibited the highest transfection efficiency (~2.2–2.3 folds vs. bPEI 25 kDa) and (~4.36–5.3 folds vs. lPEI 25 kDa) in both the cell lines. In addition, all the formulations displayed excellent cell viability (~99% vs. ~64% in bPEI and 93% in lPEI). Besides these assays, various other properties of LP-GO-2 conjugate were also assessed such as DNA binding, buffering capacity, siRNA delivery, DNA release and protection from nucleases.

2. Experimental

2.1. General

High retention dialysis tubing (cut off 12 kDa), bPEI 25 kDa, 3-(4,5-dimethylthiazol-2-yl)-2,5-diphenyltetrazolium bromide (MTT), tetramethylrhodamine isothiocyanate (TRITIC) and GFP-specific siRNA were obtained from Sigma–Aldrich Chemical Co., USA. lPEI 25 kDa was procured from Polyscience Inc., USA. YOYO-1 iodide and 4′,6-diamidino-2-phenylindole hydrochloride (DAPI) were purchased from Invitrogen Inc., USA. Bradford reagent was obtained from Bio-Rad Inc., USA. Graphene oxide was obtained from M/s. SHC International Co. Ltd., China, as a gift sample. Plasmid purification kit was purchased from Qiagen (France). Zetasizer Nano-ZS (Malvern Instruments, UK) was used to determine the particle size and zeta potential. GFP (Green Fluorescent Protein) reporter gene expression was observed under Nikon Eclipse TE-2000-S inverted microscope and the pattern in transfected cells was analyzed (excitation at 488 nm, emission at 509 nm) on NanoDrop™ ND-3300 spectrofluorometer (USA). The FTIR spectra of dried materials were recorded using the Perkin-Elmer®Spectrum™ 1000 FT-IR spectrometer (Perkin Elmer Inc., San Jose, CA) equipped with a Universal ATR (attenuated total reflectance) sampling device containing diamond crystal with following scan parameters: scan range, 4000–800 cm^{-1}; scan speed, 0.2 cm/s, accumulations at a resolution of 4 cm^{-1}. Triplicates of each sample were averaged to obtain an average spectrum. A background spectrum of air was scanned under identical conditions before each series of measurements. Thermogravimetric analysis (TGA) of GO and LP-GO conjugates was carried out on DTG-60 (Shimadzu Corp., Japan) equipped with TG units at a heating rate of 10 °C/min from 37 °C to 600 °C under nitrogen atmosphere. Intracellular trafficking studies of dual labeled LP-GO-2/pDNA complex were carried out by fluorescence microscopy (Leica DMI 6000B, Leica Microsystems, Germany).

Human embryonic kidney (HEK293) and human cervical adenocarcinoma (HeLa) cells were obtained from the cell repository facility at National Centre for Cell Sciences, Pune, India. Cell cultures were maintained (37 °C, humidified 5% CO_2–air) in Dulbecco's modified Eagle's culture medium (DMEM) (Sigma, USA) with 10% heat inactivated fetal bovine serum (FBS) (GIBCO-BRL-Life Technologies, UK) and 1% antibiotic cocktail of streptomycin and penicillin. A DNA plasmid encoding for enhanced green fluorescent protein (EGFP) was used as a model system to study LP-GO-mediated gene transfection.

2.2. Synthesis of lPEI-graphene oxide (LP-GO) conjugates

A small series of LP-GO conjugates was prepared by reacting lPEI with the epoxide functions on the GO surface at different weight ratios. A pre-heated aqueous solution of lPEI (15 mg, 1 mg/ml, for weight ratio 1.5:1) was added to a GO solution (10 mg, 0.1 mg/ml of H_2O). The mixture was sonicated for 1 h and then stirred for 12 h at 45 ± 2 °C followed by addition of saturated aqueous solution of sodium hydrogen carbonate (10 ml). After 15 min of stirring, the solution was centrifuged at 12,000*g* and the supernatant was decanted off. The residue was again suspended in hot water (50 °C, 100 ml), stirred for 15 min and centrifuged. The process was repeated twice to get rid of unreacted lPEI and the conjugate (LP-GO-1) was dried under vacuum. Likewise, LP-GO-2 and LP-GO-3 conjugates were prepared by taking 25 mg and 50 mg of lPEI, respectively, corresponding to weight ratios of 2.5:1 and 5:1,

respectively. Subsequently, formation of LP-GO conjugates was analyzed by spotting the aqueous solutions of the conjugates and GO (0.5 μl) on a glass microslide followed by visualization of the spots under a microarray laser scanner at 570 nm (laser power, 80% and PMT, 75%). Further, LP-GO-2 was also characterized by IR spectroscopy.

2.3. Gel retardation assay

LP-GO/pDNA complexes (20 μl) were prepared by mixing aqueous solutions of LP-GO (1 mg/ml) and pDNA (1 μl, 0.3 μg/μl) at various N/P ratios (8, 10, 12, 15) in 5% dextrose solution. The complexes were mixed thoroughly by vortexing and incubated for 30 min at 25 ± 2 °C. Similarly, lPEI/pDNA and bPEI/pDNA polyplexes were prepared at different N/P ratios (3, 5, 8, 12). A mixing control, GO(lPEI) in which lPEI was mixed with GO, was also complexed with pDNA at N/P ratios of 3, 5, 8 and 12. Subsequently, the pDNA complexes (20 μl) were mixed with 2 μl xylene cyanol (2.5 mg/ml, in 20% glycerol), loaded onto a 0.8% agarose gel and electrophoresed (100 V, 1 h). Then the gel was stained with ethidium bromide (EtBr) and visualized on a UV transilluminator using a Gel Documentation System (Syngene, UK).

2.4. Preparation of pDNA complexes

LP-GO/pDNA, lPEI/pDNA and bPEI/pDNA complexes were freshly prepared at different N/P ratios prior to their use. Briefly, an aqueous solution of LP-GO-1 (1 mg/ml) was added to 1 μl of pDNA (0.3 μg/μl) at various N/P ratios (10, 20, 30, 60, 95, 97, 110, 130 and 150) in 5% dextrose (5 μl) and final volume was made up to 20 μl with water. The resulting complexes were gently vortexed and incubated at 25 ± 2 °C for 30 min prior to their use in transfection experiments. Similarly, LP-GO-2 and LP-GO-3/pDNA complexes were prepared at the same N/P ratios. bPEI/pDNA, lPEI/pDNA and GO(lPEI)/pDNA complexes were prepared at N/P ratios of 10, 13, 17, 20 and 30.

2.5. Size and zeta potential measurements

The particle size and zeta potential of the pDNA complexes of LP-GO conjugates, lPEI and bPEI (prepared at their best working N/P ratios), suspended in water (1 mg/ml), were determined in pure water and complete medium by dynamic light scattering (DLS) using Zetasizer Nano-ZS. The data analysis was performed in automatic mode and the measured sizes and zeta potential (in triplicates) were presented as the average value of 20 and 30 runs, respectively. The average values of zeta potential were estimated by Smoluchowski approximation from the electrophoretic mobility.

2.6. Buffering capacity

The capability of LP-GO-2 conjugate and lPEI to resist acidification was evaluated by an acid–base titration method reported in the literature [28]. In brief, 3 mg of each sample was taken up in 0.15 N NaCl at a concentration of 0.1 mg/ml. The pH of the solutions was adjusted to 10 and then titrated by adding a solution of 0.1 N hydrochloric acid (25 μl at a time) until a pH of 3.0 was reached. A graph was plotted between pH and the amount of 0.1 N HCl consumed for bringing the pH of the solutions from 10 to 3.

2.7. Cell viability assay

To assess the toxicity of the pDNA complexes of the LP-GO conjugates and PEIs (linear and branched), MTT assay was performed spectrophotometrically at 540 nm post-36 h of transfection on HEK293 and HeLa cells. Briefly, HEK293 cells were seeded in a 96-well plate in 200 μl of DMEM supplemented with 10% FBS and allowed to grow for ~48 h. After removal of the medium, cells were treated with LP-GO/pDNA complexes (N/P ratios 10, 20, 30, 60, 75, 97, 110, 130 and 150), lPEI and bPEI/pDNA polyplexes (N/P ratios 10, 13, 17, 20 and 30). After 4 h, the medium was removed from each well and replaced by growth medium supplemented with 10% FBS. The plates were kept in an incubator (37 °C, humidified 5% CO_2 atmosphere) for 36 h, after which fresh growth medium (100 μl) containing MTT (50 μg) was added to each well. Cells were further incubated at 37 °C for 4 h. Then the supernatant was removed and formazan crystals were solubilized in 100 μl isopropanol containing 0.06 M HCl and 0.5% SDS. Finally, the absorbance was recorded at 570 nm using a Microplate Reader (Biotek, USA). Untreated cells served as control with 100% viability and wells, having MTT reagent only without cells, were used as blank to calibrate the spectrophotometer to zero absorbance. All the experiments were carried out in triplicate. Likewise, the experiment was carried out on HeLa cells. The cell viability (%) was estimated as $[abs]_{transfected}/[abs]_{control} \times 100$.

2.8. In vitro transfection

HEK293 and HeLa cells were seeded separately in 96-well plates, 24 h prior to putting transfection assay, after which the media was aspirated and cells were washed with phosphate buffered saline (1× PBS). pDNA (0.3 μg) was complexed with LP-GO conjugates, PEIs (linear and branched, 25 kDa) and GO(lPEI) control, as described under cell viability assay, and diluted with serum free DMEM (60 μl) to a final volume of 80 μl. The complexes were then gently added on to the cells. After 4 h of incubation (37 °C, humidified 5% CO_2 atmosphere), the transfection medium was aspirated, replaced by 200 μl growth medium (DMEM containing 10% FBS) and the cells further incubated for 36 h. EGFP expression in mammalian cells was quantitatively estimated on NanoDrop™ ND-3000 spectrofluorometer (USA).

2.9. Flow cytometric analysis

The transfection efficiency was also determined by quantifying the percentage of cells expressing green fluorescent protein (GFP) using flow cytometry (FACS Caliber System from GUAVA, San Joes, CA). HEK293 cells (6×10^5 cells/well) were seeded in 24-well plates and incubated at 37 °C under humidified 5% CO_2 atmosphere for 24 h in DMEM medium containing 10% FBS. LP-GO/pDNA complexes (at N/P ratios of 60, 75, 97 and 130), lPEI/pDNA and bPEI/pDNA polyplexes (at N/P ratio of 20 and 13, respectively) were prepared as described above. At the time of transfection, the medium in each well

was replaced by 300 μl of DMEM and 100 μl of pDNA complex. Cells were incubated for 4 h at 37 °C in a humidified 5% CO_2 atmosphere and then the medium was replaced by 1 ml of DMEM containing 10% FBS and the cells further incubated for 36 h. After visualizing under a fluorescence microscope, cells were separately harvested from each well by the trypsin–ethylenediaminetetraacetic acid (EDTA) treatment and suspended in 200 μl of PBS (pH 7.4). Subsequently, the cells were transferred to the cuvettes for analysis on flow cytometry. The non-transfected cells were used as a negative control.

2.10. Quantification of GFP expression

Post-transfection, the plates were observed under inverted fluorescence microscope at 10× magnification. Transfected cells were washed with 1× PBS (2 × 100 μl), treated with 50 μl lysis buffer (10 mM Tris, 1 mM EDTA and 0.5% SDS pH 7.4) and agitated for 45 min at 37 °C. Fluorescence intensity was estimated in 2 μl lysates spectroflurometrically and corrected for background and auto-fluorescence in mock-treated cells. Total protein content in cell lysate from each well was estimated using Bradford reagent (BioRad) with bovine serum albumin (BSA) (Bangalore Genei, India) as a standard. The fluorescence intensity of GFP was estimated in triplicate. Background was subtracted and expressed as arbitrary fluorescence units/mg protein.

2.11. DNA release assay

To examine the DNA binding ability of the projected LP-GO conjugates, DNA release assay was carried out and the results compared with lPEI and bPEI. Briefly, LP-GO-2/DNA, lPEI/DNA and bPEI/DNA complexes were prepared at N/P ratios of 97, 20 and 13, respectively, as described above. Afterwards, an aqueous solution of heparin (1 U/μl, an anionic polymer), was added by varying the amount from 0 to 5 U for the release of bound pDNA. The samples were then incubated for 30 min and electrophoresed (100 V, 1 h) on a 0.8% agarose gel in a TAE running buffer. The gel was stained with ethidium bromide and visualized on a UV transilluminator using a Gel Documentation System. The amount of DNA released from complexes after heparin treatment was estimated densitometrically.

2.12. DNase I protection assay

For DNase I protection assay, we prepared the solutions of pDNA (0.6 μg/25 μl) and LP-GO-2/pDNA complex (at the best working concentration). To each solution (10 μl) was added 1 μl of DNase I (1 U/μl in a buffer containing 100 mM Tris, 25 mM $CaCl_2$) and incubated for 0.25, 0.5, 1 and 2 h at 25 ± 2 °C. Samples taken up in 1× PBS served as control. After incubation, DNase I was inactivated by adding 5 μl of 100 mM EDTA for 10 min followed by incubation at 75 °C for 10 min. Heparin (10 μl, 1 U/μl) was then added to the complex and incubated for 2 h at 25 ± 2 °C to release the pDNA from the complexes. Samples were electrophoresed on a 0.8% agarose gel (100 V, 1 h), stained with ethidium bromide, visualized on a Gel Documentation System and imaged. The amount of released pDNA from complexes was determined densitometrically.

2.13. Delivery of siRNA

In order to achieve the delivery of GFP-specific siRNA to knockdown GFP expression in HEK293 cells, pDNA was complexed with LP-GO-2 at N/P ratio of 97 and transfected the cells as described above in the Section 2.8. After 3 h of exposure, the medium was aspirated, cells washed with 1× PBS (100 μl) and added 20 μl of LP-GO-2/siRNA complex (12 μg/300 ng) diluted with serum-free DMEM (60 μl) for 3 h of incubation. Then, the complex was replaced by the fresh medium containing 10% FBS (200 μl) and kept the plate in an incubator for 36 h. Transfection with LP-GO-2/pDNA was used as a control. Similarly, the assay was performed with the native lPEI. The levels of gene expression in both the cases were estimated by quantifying GFP. The assay was performed in triplicate.

2.14. Fluorescence microscopy

To monitor cellular uptake and intracellular distribution of the dual labeled LP-GO-2/pDNA complex, LP-GO-2 conjugate (0.5 ml, 5 mg/ml in H_2O) was reacted with tetramethylrhodamine isothiocyanate (TRITC, 10 μl, 0.5 mg/50 μl in DMF) to block ~1% of total amines in the conjugate. Then, the solution was concentrated and the unreacted/hydrolyzed TRITC was removed by washings with ethyl acetate (3 × 1 ml) to obtain tetramethylrhodamine-labeled LP-GO-2 (TRM-LP-GO-2). Likewise, pDNA (0.3 μg) was labeled with YOYO-1 iodide (2 μl, 1 mM solution in DMSO) and kept on stirring for 2 h at ambient temperature in dark. Then, it was stored at −20 °C. HeLa cells were seeded at ~1.5×10^5 cells/well in a 6-well plate containing coverslips and incubated for 16 h. TMR-LP-GO-2/YOYO-1-pDNA complex (0.5 ml, prepared at w/w ratio of 97) was added gently on to the cells and left for incubation for different time intervals. Then, cells were washed with 1× PBS (3 × 1 ml) followed by fixing the cells with 4% paraformaldehyde. The fixed cells were again washed with 1× PBS (3 × 1 ml). Staining of the nucleus was done by 4′,6-diamidino-2-phenylindole (DAPI) just before microscopy by incubating the cells with the dye (20 μl, 10 ng/ml) for 10 min and excess of the dye was washed of with 1× PBS (3 × 1 ml). The coverslips were mounted on the clean glass slides with fluorescence-free glycerol-based UltraCruz™ Mounting Medium (Santa-Cruz Biotechnology, USA) and examined under the fluorescence microscope.

3. Results and discussion

In the recent years, carbon-based nanomaterials have attracted tremendous attention in various fields to explore their potential applications [29–32]. Here, the major aim to undertake this study was to evaluate the efficacy of LP-GO conjugates for gene delivery. While designing the present strategy, the following points were taken into consideration, viz., (i) the protocol to synthesize LP-GO conjugates should be simple, (ii) it should evade complex chemical reactions,

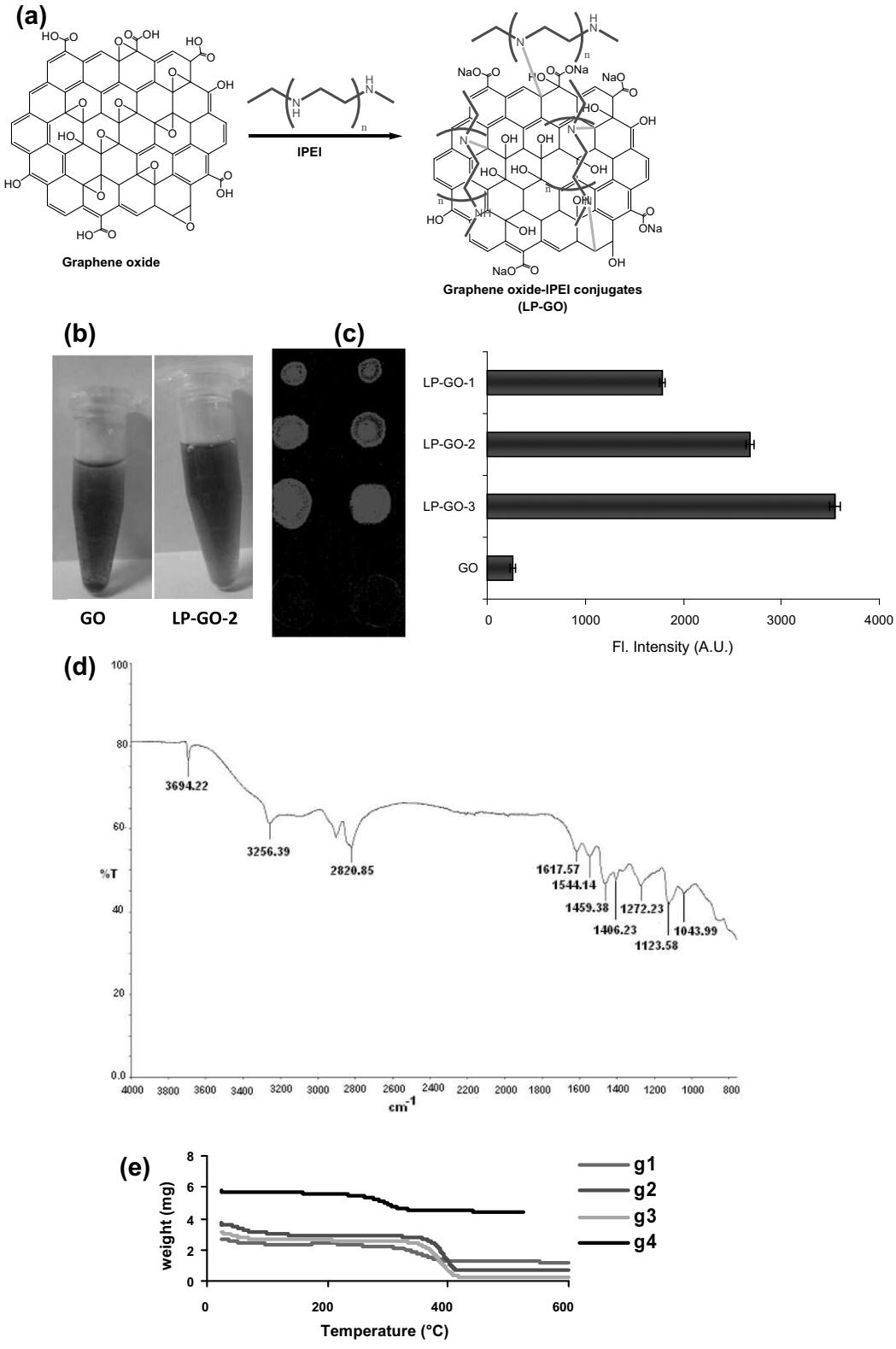

Fig. 1 – (a) Schematic representation of preparation of LP-GO conjugates. (b) Dispersibility of GO and LP-GO-2 conjugate in water after 12 h. (c) Scanned image of glass microslide spotted with GO and LP-GO conjugates in duplicate. Quantification data of the fluorescent spots is represented as bar diagram. Laser power: 80%, PMT: 75%. (d) FTIR of LP-GO-2 conjugate. Peaks at 3694 and 1044 cm^{-1} are attributed to O–H vibrations generated after reaction of GO with lPEI, while peaks at 3256 and 1124 cm^{-1} are corresponding to N–H and C–N stretching; and (e) Thermogravimetric analysis of LP-GO-1 (g1), LP-GO-2 (g2), LP-GO-3 (g3) and GO (g4). Change in the weight of sample (mg) was plotted against temperature. The weight loss ~400 °C was attributed to the decomposition of lPEI polymer.

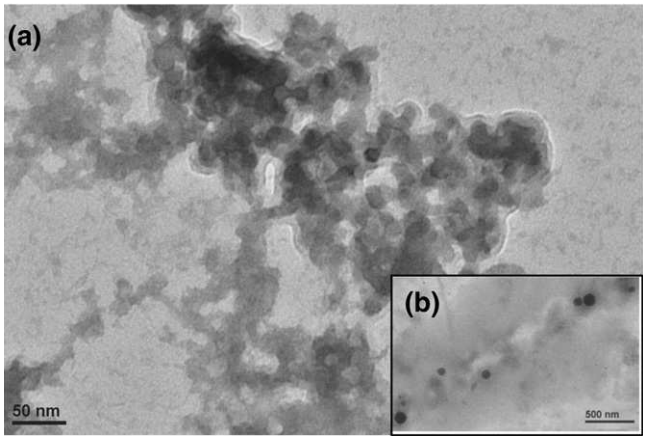

Fig. 2 – TEM images of (a) LP-GO-2 conjugate, and (b) morphology of the particles. Concentration, 1.0 mg/ml.

(iii) the projected conjugates should efficiently carry the nucleic acid therapeutics to the insides of the cells, and (iv) the conjugates should be non-toxic. Keeping these points in mind as well to address the limitations of the previous studies, we grafted lPEI on to GO surface by opening of the oxirane ring, which generated positively charged LP-GO conjugates capable of binding negatively charged pDNA through electrostatic interactions. These complexes were subsequently assessed for their toxicity and ability to deliver DNA in to the cells.

3.1. *Synthesis and characterization*

To examine the feasibility of GO as a vector to deliver nucleic acids *in vitro*, it was reacted with varying amounts of lPEI exploiting the reactivity of epoxides on its surface with the nucleophilic secondary amines of lPEI (Fig. 1a). Three different formulations, viz., LP-GO-1, LP-GO-2 and LP-GO-3, were prepared by taking different w/w ratio of lPEI:GO :: 1.5:1, 2.5:1 and 5:1, respectively. After performing purification steps, the dispersibility of the material was checked in water and DMEM containing 10% FBS, and it was found to form homogeneous solution in both the media indicating that the substitution of lPEI substantially improved the solubility of LP-GO conjugates. Fig. 1b depicts the stability of the dispersed GO and LP-GO-2 conjugate in pure water after 12 h. GO did go into water during sonication, however, due to its hydrophobic character, started precipitating out after 4 h, while LP-GO-2 conjugate remained in the solution even after 12 h of storage. Chemical formation of LP-GO conjugates was also confirmed by evaluating their optical properties. Oxidation of graphene produces GO with epoxy and carboxyl functions on its surface, which disrupt the π networks and form isolated sp^2 domains (polyaromatic clusters) in the structure. Further, the generation of such reactive groups (epoxy and carboxyls) induces non-radiative recombination of localized electron-hole pairs, which make GO a non-emissive material. Reaction of epoxy and carboxyl functions on the GO with alkylamines largely removes the non-radiative recombinative sites and transforms GO, a weak emitter of fluorescence, to its conjugates with efficient emissive property. It has also been reported that electrostatic interactions severely diminish the fluorescence of the conjugates [27]. In order to explore the fluorescent character of the LP-GO conjugates, here, aqueous solutions (0.5 μl) of GO and LP-GO conjugates were spotted on a glass microslide and after drying, it was scanned under a microarray laser scanner operating at 550 nm. Spots corresponding to GO did not fluoresce, while LP-GO conjugates exhibited fluorescence in increasing order (LP-GO-1 displayed lower fluorescence whereas LP-GO-3, bearing higher amount of amines, showed the highest intensity) indicating the covalently linked LP-GO conjugates (Fig. 1c). The larger size of the spots corresponding to LP-GO-3 might be due to greater hydrophilicity of the conjugate on the hydrophilic surface compared to LP-GO-1, which did not spread due to hydrophobicity of the conjugate. Further, LP-GO-2 conjugate was characterized by FTIR spectroscopy. Bands at 3694 and 1044 cm^{-1} confirmed the presence of hydroxyl groups while bands at 1124 and 3256 cm^{-1} accounted for C–N and N–H stretching, respectively (Fig. 1d). Quantitative estimation of lPEI conjugated to GO through epoxy functions was carried out by thermogravimetric analysis. The results revealed that at about 350 °C, GO showed ~24.27% weight loss mainly due to the loss of functional groups and at about 400 °C, LP-GO-1, LP-GO-2 and LP-GO-3 showed 39.24%, 59.95% and 73.48% weight loss, respectively (Fig. 1e). From the data, the amount of lPEI conjugated to GO was found to be ~15%, 36% and 49% in LP-GO-1, LP-GO-2 and LP-GO-3, respectively. Subsequently, these conjugates were complexed with pDNA and subjected to size and zeta potential measurements.

3.2. *Size and zeta potential measurements*

In order to determine the size and charge of the LP-GO/pDNA complexes, these were characterized by dynamic light scattering (DLS) in water and DMEM containing 10% FBS. The size of the LP-GO/pDNA complexes was found to be in nanometric range (~314 to 428 nm), which decreased in the complete medium to 111–141 nm (Table 1). All the LP-GO/pDNA and PEIs/pDNA complexes were analyzed at their best working N/P ratio (where these complexes exhibited the highest transfection efficiency), 97 for LP-GO/pDNA, 20 for lPEI/pDNA and 13 for bPEI/pDNA complexes. Zeta potential of GO in water was found to be −48.2 mV, while LP-GO conjugates showed in the range of +31.5 to +35 mV. On increasing the amount of lPEI in the conjugates (from LP-GO-1 to LP-GO-3), there was a concomitant increase in the positive charge density on the conjugates, which further confirmed the conjugation of lPEI on to GO surface (Table 1). On complexation with pDNA, zeta potential recorded a decrease due to partial neutralization of the positive charge on the LP-GO conjugates. Zeta potential of LP-GO/pDNA complexes though remained less than lPEI/pDNA complexes, it was still sufficient to interact directly with inner surface of the endosome and promote its disruption, thereby, helping in the release of LP-GO/pDNA complexes in the cytoplasm. In complete medium, the zeta potential became negative, which was in parallel to the earlier findings [33,34].

Further, the size of the LP-GO-2 particles on transmission electron microscopy was found to be in the range ~50 to 85 nm (Fig. 2). The difference in the size of nanoparticles

Table 1 – Size and zeta potential measurements.

Sample ID	Average particle size in nm ± SD (PDI)		Zeta potential in mV ± SD			Ratio of conjugate: DNA (N/P)
	DNA loaded complexes (in H_2O)	DNA loaded complexes (in complete media)	LP-GO conjugates (in H_2O)	DNA loaded complexes (in H_2O)	DNA loaded complexes (in complete media)	
LP-GO-1	428.4 ± 4.35 (0.31)	141.2 ± 2.1 (0.34)	31.5 ± 2.18	27.1 ± 2.74	−12.3 ± 3.23	97
LP-GO-2	340.2 ± 4.4 (0.32)	121.2 ± 3.3 (0.28)	33.4 ± 2.7	24.5 ± 2.9	−11.5 ± 3.1	97
LP-GO-3	314.1 ± 2.7 (0.33)	111.1 ± 3.2 (0.23)	35.2 ± 2.9	21.2 ± 3.1	−11.8 ± 2.9	97
lPEI	202.6 ± 8.2 (0.41)	136.2 ± 5.8 (0.39)	41.5 ± 4.5	36.8 ± 3.9	−15.5 ± 2.4	20
bPEI	235.3 ± 3.8 (0.49)	142.6 ± 3.9 (0.44)	42.1 ± 2.3	31.8 ± 2.2	−15.1 ± 3.5	13

recorded by DLS and TEM might be due to the fact that DLS measures the hydrodynamic diameter of the nanoparticles while in TEM, size is measured in dry state.

3.3. *Gel retardation assay*

To demonstrate the DNA binding ability of LP-GO conjugates, gel retardation assay was carried out. A mixing control was also prepared freshly in which lPEI was mixed with GO [GO(lPEI)]. LP-GO/pDNA complexes were prepared at desired N/P ratios (see Section 2) using a fixed amount of pDNA (0.3 μg) and incubated at 25 ± 2 °C for 30 min followed by loading on a 0.8% agarose gel (100 V, 1 h). The gel was visualized on a UV transilluminator and from the image, it was observed that LP-GO conjugates completely retarded the mobility of pDNA at N/P ratio of 10, lPEI and bPEI retarded the same amount of pDNA at N/P ratio of 5 (Fig. 3) and the mixing control, GO(lPEI), at 8. From these data, it was inferred that LP-GO conjugates required a higher N/P ratio than PEIs and the control, GO(lPEI), to retard the fixed amount of pDNA, which might be due to lower positive charge available on LP-GO conjugates compared to PEIs and the mixing control. This finding further confirmed the formation of LP-GO conjugates (Table 1). The mixing control, GO(PEI), also required slightly higher N/P ratio, which could be due to the partial neutralization of the charge on lPEI by carboxyl functions on GO.

3.4. *Buffering capacity*

The proton-sponge effect has been widely speculated to account for the cytosolic appearance of polyplexes like PEIs [11]. lPEI exhibits considerable buffering capacity over a pH range of 3–10 and helps in escape of pDNA from endosomes/lysosomes [16]. Fig. 4 shows the buffering capacity of LP-GO-2 (the best working sample) and lPEI in the pH range of 10–3. From this assay, it was observed that LP-GO-2 conjugate required slightly higher amount of 0.1 N HCl compared to lPEI in bringing the pH from 10 to 3. This could be due to the fact that lPEI contains only secondary amines along the length of the polymer and subsequent to its reaction with epoxides of GO, some of the secondary amines get converted into tertiary amines, which, in turn, might improve the buffering capacity of the LP-GO-2 conjugate. It has also been reported earlier from our laboratory that the conversion of secondary amines to tertiary enhances the buffering capacity of the resulting system [16]. Therefore, LP-GO-2 exhibited slightly higher buffering capacity than the lPEI, however, it is not the core parameter in deciding the transfection efficiency of the system under study [16].

3.5. *DNA release assay*

Efficient release of pDNA from the complexes is one of the pre-requisites in determining the transfection efficiency of the vector system. A vector system carrying a gene of choice inside the cell is required to release it at the desired target to facilitate efficient transfection [36]. LP-GO-2/pDNA, lPEI/pDNA and bPEI/pDNA complexes were evaluated for their DNA release ability using heparin as a polyanion to compete with pDNA to interact with the cationic polymer. The complexes were prepared at their best working N/P ratio using a fixed amount of pDNA (0.3 μg) (LP-GO-2/pDNA, N/P ratio 97;

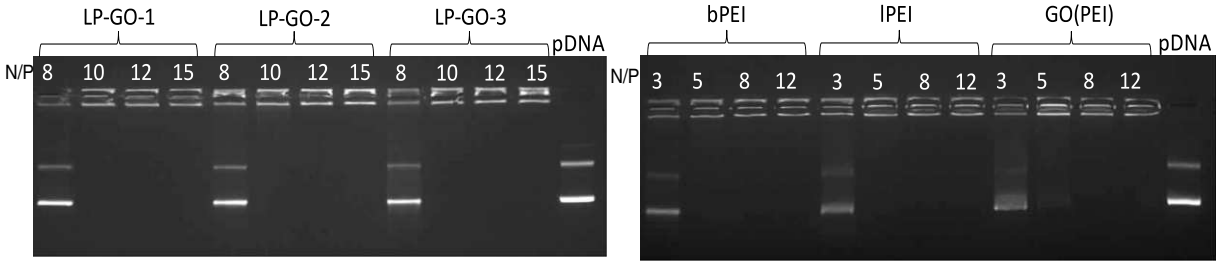

Fig. 3 – Gel retardation assay of pDNA complexes of LP-GO conjugates, lPEI and the mixing control, GO(lPEI). LP-GO/pDNA retarded the mobility of pDNA (0.3 μg) at N/P ratio of 10, PEIs/pDNA complexes at N/P ratio of 5 and GO(lPEI) at 8.

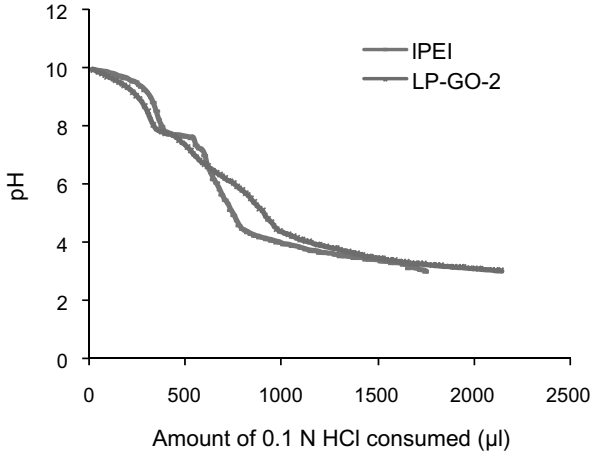

Fig. 4 – Buffering capacity of LP-GO-2 conjugate and lPEI using acid–base titration method.

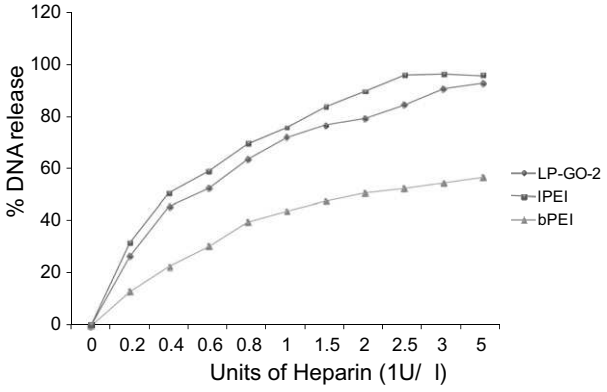

Fig. 5 – DNA release assay of LP-GO-2/pDNA, lPEI/pDNA and bPEI/pDNA complexes. Heparin was added in increasing amounts and incubated the mixtures at 25 ± 2 °C for 30 °C. The samples were run on a 0.8% agarose gel at 100 V for 1 h.

lPEI/pDNA, N/P ratio 20 and bPEI/pDNA, N/P ratio 13). The complexes, after incubation with increasing units of heparin, were run on a 0.8% agarose gel (100 V, 1 h). Densitometric analysis revealed that with 3 U of heparin, LP-GO-2/pDNA complex released up to ~90% pDNA, while bPEI and lPEI/pDNA polyplexes released ~55% and ~96% pDNA, respectively (Fig. 5). Further, on increasing the heparin concentration (5 U), the amount of pDNA released from LP-GO-2/pDNA complex was found to be ~93%, while bPEI and lPEI/DNA polyplexes released ~58% and 97% pDNA, respectively. These results clearly indicate that bPEI binds DNA very tightly and releases it poorly, while lPEI binds it very loosely, releases it before it reaches the cell. Binding of LP-GO-2 lies between bPEI and lPEI, which is neither too tight nor too loose. Hence, LP-GO-2 conjugate possesses the capability to carry DNA through the cellular barriers and release it timely in the cellular milieu.

3.6. *Cell viability assay*

Prior to exploring the gene transfer ability of the LP-GO conjugates, cell viability properties of the conjugates were

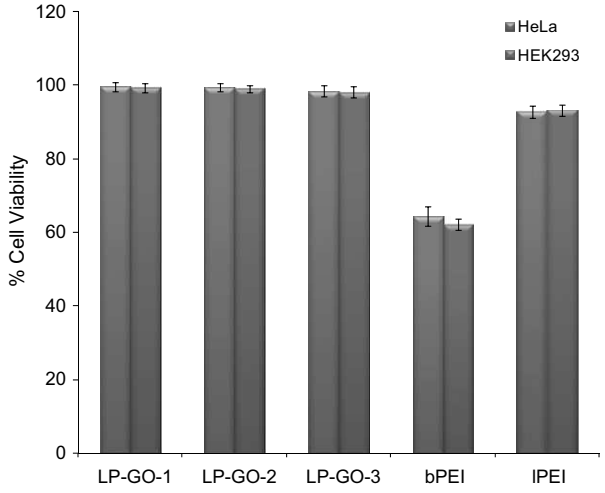

Fig. 6 – Cell viability assay of LP-GO/DNA, bPEI/DNA and lPEI/DNA complexes on HEK293 and HeLa cells. The assay was carried out in triplicate and each point represents the mean of three independent experiments.

examined on HEK293 and HeLa cells. Mainly, cytotoxicity of the cationic polymers arises due to the aggregation of these polymers on the cell surface impairing the important membrane function like protein kinase activity [35]. In order to assess the cell viability of LP-GO/pDNA complexes, MTT assay was performed and the results were compared with lPEI/pDNA and bPEI/pDNA complexes. Untreated cells were considered as positive control and their cell viability set as 100%. Fig. 6 shows the results of the cell viability assay. From the results, it was observed that LP-GO/pDNA complexes exhibited significantly higher cell viability (~98% to 100%) compared to that observed in bPEI/DNA complex (~64%). lPEI/DNA complex, on the other hand, displayed non-significant cytotoxicity (~5% to 7%) in the tested cell lines (Fig. 6). From the data, it was inferred that on conjugation of non-toxic lPEI to GO surface, there was a slight decrease in the zeta potential of the conjugates compared to lPEI (Table 1) due to charge conversion from secondary to tertiary amines and this could be the reason for displaying higher cell viability by LP-GO conjugates. Moreover, this assay also revealed that on increasing the amount of lPEI in the conjugates from LP-GO-1 to LP-GO-3, positive charge on the conjugates also increased (Table 1), however, this increase in positive charge did not result in the significant change in the cell viability of the conjugates down the group. Therefore, higher cell viability of LP-GO/DNA complexes renders them to be suitable as gene delivery vectors for *in vivo* applications.

3.7. *In vitro transfection*

Having evaluated LP-GO/DNA complexes as non-toxic to the cells, these were subsequently examined for their ability to deliver pDNA into the mammalian cells *in vitro*. Transfection was carried out on HEK293 and HeLa cells with pDNA complexes of LP-GO conjugates, PEIs (linear and branched, 25 kDa) and a mixing control, GO(lPEI), at different N/P ratios. After 36 h of incubation, the cells were observed under a

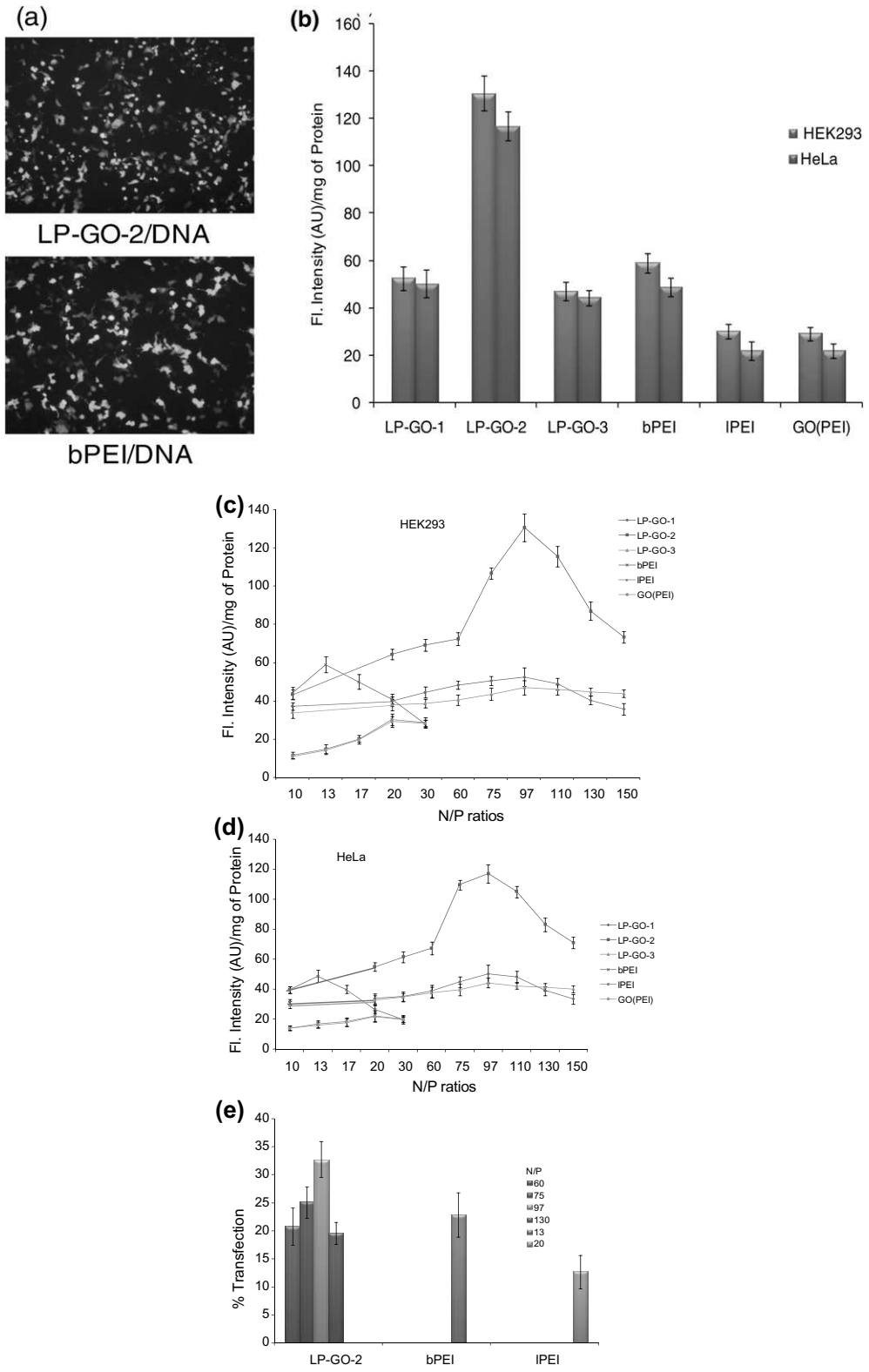

Fig. 7 – (a) Fluorescence microscopic images of HEK293 cells transfected with bPEI/pDNA and LP-GO-2/DNA complexes at N/P ratios of 12 and 97, respectively. Cells transfected with respective pDNA complexes were observed under UV, C-F1 epifluorescence filter of fluorescence microscope. Images were recorded at 10× magnification. (b) Transfection efficiency of LP-GO/pDNA, lPEI/pDNA, bPEI/pDNA and GO(lPEI)/pDNA complexes at optimal N/P ratio. (c) Dose dependent transfection efficiency of the above formulations at various N/P ratios on HEK293 cells. (d) Dose dependent transfection efficiency of the above formulations at various N/P ratios on HeLa cells. (e) Percent transfection efficiency of LP-GO-2/DNA, lPEI/DNA and bPEI/DNA complexes at various N/P ratios, as determined by FACS.

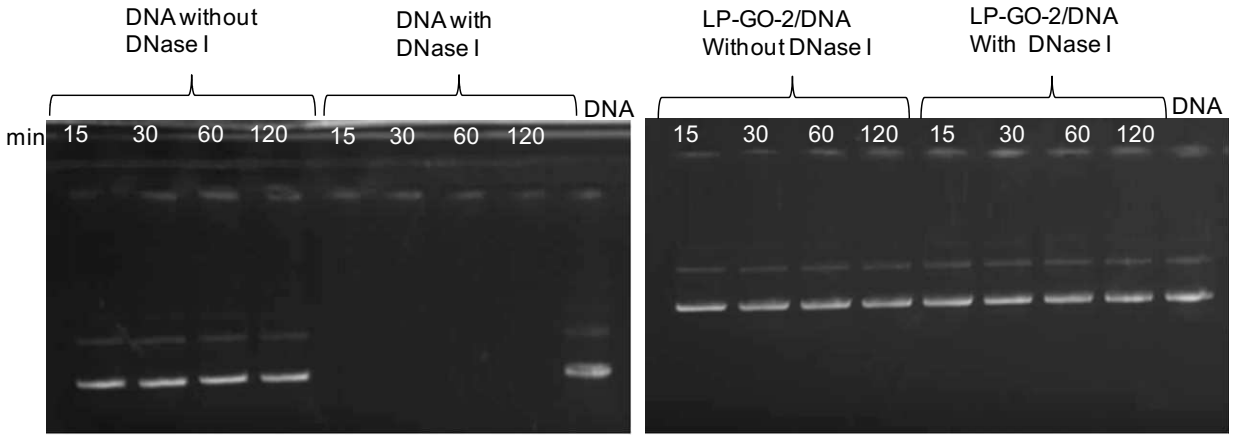

Fig. 8 – DNase I protection assay of LP-GO-2/DNA complex treated with DNase I for different time intervals. Addition of heparin released the complexed DNA and the amount of DNA protected (%) was calculated as the relative integrated densitometry values (IDV), quantified and normalized by that of pDNA values (without DNase I) using gel documentation system.

fluorescence microscope and the images recorded (Fig. 7a). Among all the formulations, LP-GO/pDNA complexes showed significantly higher gene transfection efficacy with LP-GO-2/pDNA complex displaying the highest transfection efficiency compared to LP-GO-1/pDNA, LP-GO-3/pDNA, lPEI/pDNA, bPEI/pDNA and GO(lPEI)/pDNA complexes in both the cell lines. The same formulation exhibited ~5.3 and ~2.3 folds higher transfection efficiency than lPEI/pDNA and bPEI/pDNA complexes, respectively (Fig. 7b), in HeLa cells. In HEK293 cells, it was found to be ~4.36 and ~2.2 folds higher than lPEI/pDNA and bPEI/pDNA complexes, respectively. The mixing control, GO(lPEI), employed in the study behaved more or like lPEI as only a few amino functions might get involved in the electrostatic interactions with the carboxyl functions on the GO surface. On performing the transfection assay at different N/P ratios (dose dependent assay) in HEK293 and HeLa cells, it was also observed that transfection efficiency initially increased with increasing the N/P ratio of LP-GO/DNA complexes and after attaining the maximum at N/P ratio of 97, it decreased thereafter (Fig. 7c and d). Likewise, lPEI/pDNA, bPEI/pDNA and GO(lPEI)/pDNA showed the highest transfection efficiency at N/P ratio of 20, 13 and 20, respectively. Transfection efficiency of LP-GO/pDNA complexes was also found to be cell-specific, i.e. out of the two cell lines used in the study, transfection efficiency was found to be higher in HEK293 (Fig. 7b–d). Conclusively, conjugation of lPEI onto GO backbone led to the generation of transfection reagents with considerably improved transfection efficiency than the native polymers, lPEI and bPEI. The later one has been reported as a gold standard in gene delivery.

Quantification of EGFP expression in the cells was also carried out using fluorescence-activated cell sorting (FACS). The analysis was performed on HEK293 cells transfected with LP-GO-2/DNA complex at different N/P ratios using pEGFP expressing vector. The results were compared with that obtained on transfection with lPEI/DNA and bPEI/DNA complexes. Non-transfected cells were used as negative control. It was observed that the transfection efficiency reached up to ~32.8 ± 3.2% for the best working LP-GO-2/pDNA complex at N/P ratio of 97, while ~22.9 ± 4% and ~12.7 ± 3% GFP positive cells were scored by the other reagents, bPEI/DNA (at N/P ratio of 13) and lPEI/DNA complexes (at N/P ratio of 20), respectively (Fig. 7e).

3.8. *DNA protection assay*

Further, to explore the ability of the LP-GO-2 conjugate to provide protection to bound DNA against nucleases, DNase I protection assay was performed by incubating LP-GO-2/DNA complex with DNase I at different time points (15, 30, 60 and 120 min). Complete degradation of free pDNA (0.3 μg) was observed within 15 min, while the conjugate, LP-GO-2, effectively protected complexed pDNA (Fig. 8) and ~86% pDNA was found to be recovered after 30 min and ~76% after 2 h of incubation with the enzyme. Thus, LP-GO-2 conjugate provided sufficient protection to bound pDNA against DNase I for a considerable time period thereby showing its potential for *in vivo* administration of nucleic acid-based therapeutics.

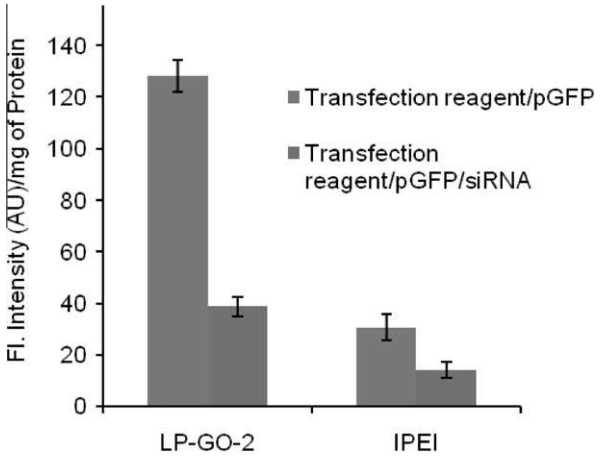

Fig. 9 – Delivery of siRNA by LP-GO-2 conjugate in HEK293 cells in comparison with lPEI/pDNA/siRNA. The experiment was carried out in triplicate.

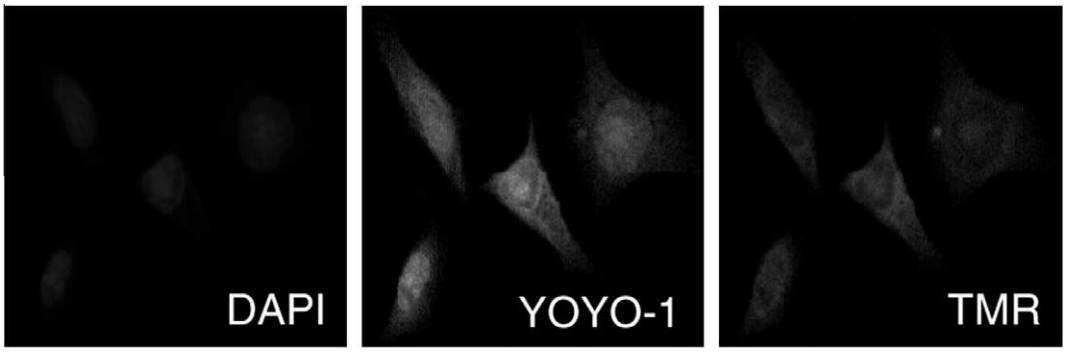

Fig. 10 – Fluorescence microscopy images of HeLa cells treated with TMR-LP-GO-2/YOYO-1-pDNA complex for 1.0 h. Nucleus was stained with DAPI and the cells observed under different filters.

3.9. *Delivery of siRNA*

In an attempt to demonstrate the versatility of the developed conjugates for the delivery of siRNA, the GFP-specific siRNA was delivered in sequential manner in HEK293 cells and the suppression of the target gene was observed quantitatively by spectrofluoremetrically. In the sequential delivery, transfection assay was first performed with LP-GO-2/pDNA complex for 3 h followed by with LP-GO-2/siRNA complex for 3 h. After 36 h of incubation, a significant knockdown of GFP expression (~69.8%) was noticed in case of LP-GO-2/pDNA/siRNA, while ~54% knockdown was observed when lPEI/pDNA/siRNA complex was used (Fig. 9). These results demonstrate the potential of the conjugate as efficient carrier of nucleic acids *in vitro*.

3.10. *Fluorescence microscopy*

In order to demonstrate the internalization and intracellular localization of dual labeled LP-GO-2/pDNA complex in HeLa cells, fluorescence microscopy was performed. Cells were treated with TMR-LP-GO-2/YOYO-1-pDNA complex (prepared at the best N/P ratio) for various time periods and after usual processing, the cells were observed under a fluorescence microscope. It was observed that after 30 min of exposure, relatively a few particles were seen in the nucleus with majority of the particles in the cytoplasm, however, post-1 h of treatment, sufficient amount of red and green fluorescence was observed inside the nucleus, which was stained by DAPI exhibiting blue fluorescence to distinguish from green and red fluorescence shown by pDNA and the conjugate, respectively (Fig. 10). A significant amount of particles entered the nucleus indicating the potential of LP-GO-2 conjugate to carry pDNA to the nucleus of the cell. The results advocate the efficacy of the conjugate for non-viral nucleic acid delivery.

4. Summary

An efficient gene delivery system based on graphene oxide chemically-functionalized with a non-toxic linear PEI (LP-GO) is reported. Linear PEI grafted GO conjugates, prepared in the present study with net positive charge density, efficiently condensed pDNA and delivered it to the insides of the cells. One of the formulations, LP-GO-2/pDNA complex, could exhibit transfection efficiency several folds higher than lPEI, bPEI and GO(lPEI) with cell viability even higher than lPEI. Besides, LP-GO-2 also showed the capability to deliver siRNA efficiently into the cells. Promising results altogether imply the potential of LP-GO conjugate as efficient non-viral gene delivery vector for future gene therapy applications.

Acknowledgements

Financial support from in-house project, EXP002, is gratefully acknowledged. Authors also thank Prof. S. Kukreti, Department of Chemistry, University of Delhi, Delhi, for his help in characterization of the conjugates.

REFERENCES

[1] Walther W, Stein U. Viral vectors for gene transfer. Drugs 2000;60:249–71.
[2] Christian AF, Kevin GR. Engineered nanoscaled polyplex gene delivery systems. Mol Pharm 2009;6:1277–89.
[3] Louis CS, Duguid J, Wadhwa MS, Logan MJ, Tung CH, Edwards V, et al. Synthetic peptide-based DNA complexes for non-viral gene delivery. Adv Drug Deliv Rev 1998;30:115–31.
[4] Jianjun Z, Yugugo L, Anandika D, Quinn KTN, Juanjuan D, Ming Y, et al. Protein–polymer nanoparticles for non-viral gene delivery. Biomacromolecules 2011;12:1006–14.
[5] Davis ME. Non-viral gene delivery systems. Curr Opin Biotechnol 2002;13:128–31.
[6] Tiera MJ, Winnik FM, Fernandes JC. Synthetic and natural polycations for gene therapy: state of the art and new perspectives. Curr Gene Ther 2006;6:59–71.
[7] Li S, Huang L. Non-viral gene therapy: promises and challenges. Gene Ther 2000;7:31–4.
[8] Troiber C, Wagner E. Nucleic acid carriers based on precise polymer conjugates. Bioconjug Chem 2011;22:1737–52.
[9] Christopher M, Wiethoff C, Middaugh R. Barriers to non-viral gene delivery. J Pharm Sci 2003;92:203–17.
[10] Kichler A, Leborgne C, Coeytaux E, Danos O. Polyethylenimine-mediated gene delivery: a mechanistic study. J Gene Med 2001;3:135–44.
[11] Sonawane ND, Szoka Jr FC, Verkman AS. Chloride accumulation and swelling in endosomes enhances DNA transfer by polyamine–DNA polyplexes. J Biol Chem 2003;278:44826–31.

[12] Akinc A, Thomas M, Klibanov AM, Langer R. Exploring polyethylenimine-mediated DNA transfection and the proton sponge hypothesis. J Gene Med 2005;7:657–63.
[13] Wightman L, Kircheis R, Rossler V, Carotta S, Ruzicka R, Kursa M, et al. Different behavior of branched and linear polyethylenimine for gene delivery in vitro and in vivo. J Gene Med 2001;3:362–72.
[14] Fischer D, Li Y, Ahlemeyer B, Krieglstein J, Kissel T. In vitro cytotoxicity testing of polycations: influence of polymer structure on cell viability and hemolysis. Biomaterials 2003;24:1121–31.
[15] Seib FP, Jones AT, Duncan R. Comparison of the endocytic properties of linear and branched PEIs, and cationic PAMAM dendrimers in B16f10 melanoma cells. J Control Release 2007;117:291–300.
[16] Goyal R, Tripathi SK, Tyagi S, Sharma A, Ram KR, Chowdhuri DK, et al. Linear PEI nanoparticles: efficient pDNA/siRNA carriers in vitro and in vivo. Nanomedicine 2012;8:167–75.
[17] Nimesh S, Goyal A, Pawar V, Jayaraman S, Kumar P, Chandra R, et al. Polyethylenimine nanoparticles as efficient transfecting agents for mammalian cells. J Control Release 2006;110:457–68.
[18] Walker GF, Fella C, Pelisek J, Fahrmeir J, Boeckle S, Ogris M. Toward synthetic viruses: endosomal pH triggered deshielding of targeted polyplexes greatly enhances gene transfer in vitro and in vivo. Mol Ther 2005;11:418–25.
[19] Tripathi SK, Goyal R, Gupta KC. Surface modification of crosslinked dextran nanoparticles influences transfection efficiency of dextran–polyethylenimine nanocomposites. Soft Matter 2011;7:11360–71.
[20] Lee DY, Khatun Z, Lee J-H, Lee Y-K, In I. Blood compatible graphene/heparin conjugate through noncovalent chemistry. Biomacromolecules 2011;12:336–41.
[21] Choi BG, Park H, Park TJ, Yang MH, Kim JS, Jang SY, et al. Solution chemistry of self-assembled graphene nanohybrids for high-performance flexible biosensors. ACS Nano 2010;4:2910–8.
[22] Dreyer DR, Park S, Bielawski CW, Ruoff RS. The chemistry of graphene oxide. Chem Soc Rev 2010;39:228–40.
[23] Pan Y, Bao H, Sahoo NG, Wu T, Li L. Water-soluble poly(*N*-isopropylacrylamide)–graphene sheets synthesized via click chemistry for drug delivery. Adv Funct Mater 2011;21:2754–63.
[24] Liu Z, Robinson JT, Sun XM, Dai HJ. PEGylated nanographene oxide for delivery of water-insoluble cancer drugs. J Am Chem Soc 2008;130:10876–7.
[25] Feng L, Zhang S, Liu Z. Graphene based gene transfection. Nanoscale 2011;3:1252–7.
[26] Chen B, Liu M, Zhang L, Huang J, Yao J, Zhang Z. Polyethylenimine-functionalized graphene oxide as an efficient gene delivery vector. J Mater Chem 2011;21:7736–41.
[27] Kim H, Namgung R, Singha K, Oh IK, Kim WJ. Graphene oxide–polyethylenimine nanoconstruct as a gene delivery vector and bioimaging tool. Bioconjug Chem 2011;22:2558–67.
[28] Swami A, Kurupati RK, Pathak A, Singh Y, Kumar P, Gupta KC. A unique and highly efficient non-viral DNA/siRNA delivery system based on PEI-bisepoxide nanoparticles. Biochem Biophys Res Commun 2007;362:835–41.
[29] Sanz V, Tîlmacîu C, Soula B, Flahaut E, Coley HM, Silva SRP, et al. Chloroquine-enhanced gene delivery mediated by carbon nanotubes. Carbon 2011;49:5348–58.
[30] Jung D-H, Kim BH, Lim YT, Kim J, Lee SY, Jung H-T. Fabrication of single-walled carbon nanotubes dotted with Au nanocrystals: potential DNA delivery nanocarriers. Carbon 2010;48:1070–8.
[31] Vashist SK, Zheng D, Pastorin G, Al-Rubeaan K, Luong JHT, Sheu F-S. Delivery of drugs and biomolecules using carbon nanotubes. Carbon 2011;49:4077–97.
[32] Ittisanronnachai S, Orikasa H, Inokuma N, Uozu Y, Kyotani T. Small molecule delivery using carbon nano-test-tubes. Carbon 2008;46:1361–3.
[33] Gabrielson NP, Pack DW. Acetylation of polyethylenimine enhances gene delivery via weakened polymer/DNA interactions. Biomacromolecules 2006;7:2427–35.
[34] Simoes S, Slepushkin V, Pires P, Gaspar R, Lima PMC, Duzgu N. Human serum albumin enhances DNA transfection by lipoplexes and confers resistance to inhibition by serum. Biochim Biophys Acta 2000;1463:459–69.
[35] Kircheis R, Wightman L, Wagner E. Design and gene delivery activity of modified polyethylenimines. Adv Drug Deliv Rev 2001;53:341–58.
[36] Benns JM, Choi JS, Mahato RI, Park JS, Kim SW. pH sensitive cationic polymer gene delivery vehicle: *N*-Ac-poly(L-histidine)-graft-poly(L-lysine) comb-shaped polymer. Bioconjug Chem 2000;11:637–45.